NATIONAL ADVISORY COMMITTEE FOR AERONAUTICS

TECHNICAL NOTE 3849

ANALYTICAL DETERMINATION OF THE NATURAL COUPLED FREQUENCIES AND MODE SHAPES AND THE RESPONSE TO OSCILLATING FORCING FUNCTIONS OF TANDEM HELICOPTERS

By George W. Brooks and John C. Houbolt

Langley Aeronautical Laboratory
Langley Field, Va.

NACA

Washington

December 1956

NATIONAL ADVISORY COMMITTEE FOR AERONAUTICS

TECHNICAL NOTE 3849

ANALYTICAL DETERMINATION OF THE NATURAL COUPLED FREQUENCIES AND MODE SHAPES AND THE RESPONSE TO OSCILLATING FORCING FUNCTIONS OF TANDEM HELICOPTERS

By George W. Brooks and John C. Houbolt

SUMMARY

A method is presented for the analytical determination of the natural coupled frequencies and mode shapes of vibrations in the vertical plane of tandem helicopters. The coupled mode shapes and frequencies are then used to calculate the response of the helicopter to applied oscillating forces. Degrees of freedom included in the analysis are translation, pitching, and bending of the fuselage; translation, flapping, and bending of the blades; and translation of the engine. The method employs the Lagrange dynamical equations for free vibrations in conjunction with the kinetic and potential energies of the system in order to obtain the differential equations of motion for the coupled system which are then written in matrix form. The elements of the determinant of the matrix equation include the natural frequencies, mode shapes, and mass distributions of the uncoupled components of the helicopter (such as fuselage, blades, and engine) and permit the inclusion of experimental data of the uncoupled components in the evaluation of the coupled frequencies of the coupled system.

The results of calculations made for a particular tandem helicopter show the variation of the coupled frequencies with rotor speed and indicate the changes in the coupled frequencies which result from changes in the structural properties of the individual helicopter components. Calculated response curves show how the vibrations of the cockpit vary with the frequency and method of application of oscillating forces applied at the hubs. Suggestions for further refinement of the analysis to aid in the determination of the coupled frequencies for more complex and realistic systems are also presented.

INTRODUCTION

In many cases the development of the prototype of a particular helicopter is handicapped because severe structural vibrations are encountered.

Such vibrations often limit the utilization of production articles because of fatigue of the component parts of the structure as well as of the operating personnel. Available information indicates that the high levels of vibration are attributable primarily to two factors; namely, the high periodic content of the aerodynamic loading on the rotor blades and the amplification of the structural deformations due to proximity of resonance. Accordingly, it appears that the vibration levels may be reduced either by reducing the levels of the oscillating aerodynamic loads, by the inclusion of appropriate damping, or by choosing the natural frequencies of the coupled structure so that they are as far as possible from the integral multiples of the rotor speed.

The present paper relates to resonance amplification and, in particular, to the determination of the natural frequencies, mode shapes, and response of the coupled helicopter structure as it exists in flight. Conventional methods such as those of references 1 and 2 may be used to predict the natural frequencies of the various components of helicopters such as fuselages, blades, and engines. Reference 3, which reports on the initial part of the present investigation, presents a method for the prediction of the natural frequencies and mode shapes of the structure which result when the various components are coupled together. The purpose of this paper is to elaborate on reference 3 and to present a method for utilizing the resulting coupled frequencies and mode shapes in computing the response of the helicopter to applied oscillating loads.

The method is an energy method that involves chosen modes and frequencies of the uncoupled components which may be determined either by expressing the potential energy of the components in terms of given stiffness and mass distributions or, preferably, from experimental vibration tests of the components. The method is given in terms of a tandem-helicopter configuration but other configurations can be treated in an analogous manner.

The present paper is concerned primarily with vibrations in the vertical plane - in particular, with fuselage translation, pitching, and bending; rotor blade translation, flapping, and bending; and engine translation. The characteristic frequency determinant is derived, and calculated values for the natural coupled frequencies and mode shapes for a particular tandem helicopter are presented. These mode shapes and frequencies are then used to determine the vibration amplitudes of the cockpit which occur when oscillating forces are applied at the front and rear rotor hubs. The results of some trend studies are also presented to show the effect of variations of the uncoupled frequency of the fuselage and of the Southwell coefficient of the rotor blades on the coupled frequencies of the helicopter.

SYMBOLS

a_0, a_1	coefficients of front-rotor-blade modal deflections $\frac{r_F}{R_F}$ and x_1, respectively, in.
A_0, A_1, B_0, B_1, C_0, C_1, D_0, D_1	coefficients of frequency determinant (defined after eq. (11))
b_0, $\bar{b}_0$, b_1	coefficients of fuselage modal deflections 1, $\frac{s}{l}$, and y_1, respectively, in.
c_0, c_1	coefficients of rear-rotor-blade modal deflections $\frac{r_R}{R_R}$ and z_1, respectively, in.
EI	structural stiffness of helicopter at station σ, lb-in.^{2}
$(EI)_F$	structural stiffness of front rotor blades, lb-in.^{2}
$(EI)_R$	structural stiffness of rear rotor blades, lb-in.^{2}
$(EI)_f$	structural stiffness of fuselage, lb-in.^{2}
F	applied forcing function (see eq. (12)), lb
F_0	amplitude of applied forcing function
g_h	structural damping coefficient
k	radius of gyration of mass of fuselage about front rotor hub, in.
K_e	spring constant for engine mounts, lb/in.
$K_{F,1}$, $K_{R,1}$	Southwell coefficients for blade first elastic flapwise bending mode (defined after eq. (11))
l	distance between front and rear rotors, in.

l_{cg}	distance from front rotor hub to center of gravity of fuselage, in.
l_e	distance from front rotor hub to engine, in.
L	overall length of helicopter, in.
m	mass per unit length of helicopter at station σ, lb-sec^2/in.^{2}
m_F	mass per unit length of front rotor blade, lb-sec^2/in.^{2}
m_R	mass per unit length of rear rotor blade, lb-sec^2/in.^{2}
m_f	mass per unit length of fuselage, lb-sec^2/in.^{2}
M_F	mass of front rotor blade, lb-sec^2/in.
M_R	mass of rear rotor blade, lb-sec^2/in.
M_e	mass of engine, lb-sec^2/in.
M_f	mass of fuselage, lb-sec^2/in.
$M_{f,1}$	effective mass of fuselage (defined after eq. (11)), lb-sec^2/in.
M_r	effective mass of helicopter in rth mode (see eq. (17)), lb-sec^2/in.
p, q	number of blades on front and rear rotor, respectively
P_r, Q_r	real and imaginary parts of response of helicopter in rth mode (see eqs. (23) and (24)), in.
r_F	radial position of any blade element on front rotor (see fig. 1), in.
r_R	radial position of any blade element on rear rotor (see fig. 1), in.
R_F	radius of front rotor, in.
R_R	radius of rear rotor, in.

s	longitudinal position of any fuselage element (see fig. 1), in.
t	time, sec
T	centrifugal force on blade at any radial station, lb; kinetic energy, lb-in.
T_F, T_R	centrifugal force on front and rear rotor blades, respectively, lb
$\overline{T}_F$, $\overline{T}_R$	centrifugal force divided by square of rotor speed, lb-sec^2
V	potential energy, lb-in.
w	deflection of engine, in.
w_f	deflection of engine with respect to fuselage, in.
x	deflection of element of front rotor blade, in.
x_1	uncoupled first-bending-mode shape for front rotor blade
X, Y	real and imaginary parts of response of helicopter (see eq. (26)), in.
y	deflection of element of fuselage, in.
y_1	uncoupled first-bending-mode shape for fuselage
z	deflection of element of rear rotor blade, in.
z_1	uncoupled first-bending-mode shape for rear rotor blade
α_r	coefficient of deflection of rth coupled mode of helicopter (see eqs. (13) and (23)), in.
$\alpha_{r,0}$	amplitude of α_r, in.
σ	distance measured rearward from leading edge of front rotor disk (see fig. 1), in.
σ_A	value of σ where oscillating force is applied

ϕ	deflection of helicopter in response to applied force F (see eqs. (13) and (25)), in.
ϕ_r	rth-coupled-mode shape of helicopter
$\lvert\phi\rvert$	amplitude of ϕ (see eq. (26)), in.
ω	natural frequency of coupled modes; frequency of applied oscillating force, radians/sec
$\omega_{F,1}$, $\omega_{R,1}$	first natural uncoupled flapwise bending frequency of front and rear rotor blades, respectively, radians/sec
$\omega_{f,1}$	first natural uncoupled vertical bending frequency of fuselage, radians/sec
ω_e	natural vertical frequency of engine on its mounts, radians/sec
ω_r	natural frequency of rth coupled mode of helicopter, radians/sec
Ω	rotor speed, radians/sec

The deflection in the first bending mode of the fuselage, measured at station s, is denoted by $y_1(s)$. For example, $y_1(0)$ is the deflection of the fuselage in first mode bending at the front rotor hub. (See fig. 1.)

ANALYSIS

Equations for Free Vibrations

General considerations.- The analysis presented in this portion of the paper deals with the determination of the undamped, natural coupled frequencies of the vertical vibrations of a tandem helicopter. The following degrees of freedom are considered: vertical translation, longitudinal pitching, and structural bending of the fuselage; vertical translation, flapping, and flapwise bending of the rotor blades on the front and rear rotors; and vertical translation of the engine. This analysis does not treat fuselage side bending and torsion; however, an analysis of the structure for side bending and torsion can be made in a manner parallel to the present analysis. Although the analysis is given in terms of a tandem helicopter configuration, other configurations may be treated in an analogous manner.

The method follows the Lagrange energy-equation approach wherein the derivation of the equations of motion consists of writing the kinetic and potential energies of the structure in terms of the displacements w, x, y, and z. (See fig. 1.) These displacements are in terms of generalized coordinates and chosen uncoupled modes of the structural components (fuselage, rotor blades, and engine). The energy equations are substituted in Lagrange's dynamical equations for free vibrations to obtain the equations of motion which yield the coupled frequencies and mode shapes.

Energy equations.- The kinetic energy T and the potential energy V are, respectively,

$$T = \frac{1}{2}\int_0^{l} m_f\left(\frac{dy}{dt}\right)^2 ds + \frac{1}{2}M_e\left(\frac{dw}{dt}\right)^2 + \frac{p}{2}\int_0^{R_F} m_F\left(\frac{dx}{dt}\right)^2 dr_F + \frac{q}{2}\int_0^{R_R} m_R\left(\frac{dz}{dt}\right)^2 dr_R \tag{1}$$

and

$$V = \frac{1}{2}\int_0^{l} (EI)_f\left(\frac{d^2y}{ds^2}\right)^2 ds + \frac{1}{2}K_e\left[w - y(l_e)\right]^2 + \frac{p}{2}\int_0^{R_F} (EI)_F\left(\frac{d^2x}{dr_F^2}\right)^2 dr_F + \frac{q}{2}\int_0^{R_R} (EI)_R\left(\frac{d^2z}{dr_R^2}\right)^2 dr_R + \frac{p}{2}\int_0^{R_F} T_F\left(\frac{dx}{dr_F}\right)^2 dr_F + \frac{q}{2}\int_0^{R_R} T_R\left(\frac{dz}{dr_R}\right)^2 dr_R \tag{2}$$

Special attention is called to the fact that the energies of the front rotor with p-blades may be different from those of the rear rotor with q-blades. For this reason, in the derivation of the energies, the deflections of the front and rear rotor blades are denoted independently by x and z, respectively. It is assumed in the present analysis that all the blades on a given rotor behave in a similar manner; however, equations (1) and (2) are readily extended to treat each blade as an independent degree of freedom.

Choice of modes.- The next step toward obtaining the differential equations of motion is to express the deflections w, x, y, and z in

terms of chosen mode shapes. The choice of the translation mode, the pitching mode, and one bending mode for the fuselage; the flapping mode and one flapwise bending mode for the blades on each rotor; and one translation mode for the engine leads to the following equations for the deflections:

For engine translation:

$$w = b_0 + \bar{b}_0 \frac{l_e}{l} + b_1 y_1(l_e) + w_f \tag{3}$$

For front-rotor-blade translation, flapping, and bending:

$$x = b_0 + b_1 y_1(0) + a_0 \frac{r_F}{R_F} + a_1 x_1 \tag{4}$$

For fuselage translation, pitching, and bending:

$$y = b_0 + \bar{b}_0 \frac{s}{l} + b_1 y_1 \tag{5}$$

For rear-rotor-blade translation, flapping, and bending:

$$z = b_0 + \bar{b}_0 + b_1 y_1(l) + c_0 \frac{r_R}{R_R} + c_1 z_1 \tag{6}$$

where the coefficients a_0, a_1, b_0, $\bar{b}_0$, b_1, c_0, c_1, and w_f are unknown functions of time, and x_1, y_1, and z_1 are the chosen spatial functions or mode shapes. If higher modes are desired, it is only necessary to add appropriate terms to equations (3) to (6).

Substitution of equations (3) to (6) into equations (1) and (2) leads to the following equations for the kinetic and potential energies, respectively:

$$T = \frac{1}{2}\int_0^l m_f\left(\dot{b}_0 + \dot{\bar{b}}_0\frac{s}{l} + \dot{b}_1 y_1\right)^2 ds + \frac{1}{2}M_e\left[\dot{b}_0 + \dot{\bar{b}}_0\frac{l_e}{l} + \dot{b}_1 y_1(l_e) + \dot{w}_f\right]^2 +$$

$$\frac{p}{2}\int_0^{R_F} m_F\left[\dot{b}_0 + \dot{b}_1 y_1(0) + \dot{a}_0\frac{r_F}{R_F} + \dot{a}_1 x_1\right]^2 dr_F +$$

$$\frac{q}{2}\int_0^{R_R} m_R\left[\dot{b}_0 + \dot{\bar{b}}_0 + \dot{b}_1 y_1(l) + \dot{c}_0\frac{r_R}{R_R} + \dot{c}_1 z_1\right]^2 dr_R \tag{7}$$

and

$$V = \frac{1}{2}\int_0^l (EI)_f(b_1 y_1'')^2 ds + \frac{1}{2}K_e(w_f)^2 + \frac{p}{2}\int_0^{R_F}(EI)_F(a_1 x_1'')^2 dr_F +$$

$$\frac{q}{2}\int_0^{R_R}(EI)_R(c_1 z_1'')^2 dr_R + \frac{p}{2}\int_0^{R_F} T_F\left(\frac{a_0}{R_F} + a_1 x_1'\right)^2 dr_F +$$

$$\frac{q}{2}\int_0^{R_R} T_R\left(\frac{c_0}{R_R} + c_1 z_1'\right)^2 dr_R \tag{8}$$

where the dots denote derivatives with respect to time and the primes denote derivatives with respect to space or length.

After the energies have been calculated, the next step is to apply Lagrange's equation for free vibration to obtain the differential equations of motion; that is,

$$\left.\begin{aligned} \frac{d}{dt}\left(\frac{\partial T}{\partial \dot{a}_0}\right) - \frac{\partial T}{\partial a_0} + \frac{\partial V}{\partial a_0} &= 0 \\ \frac{d}{dt}\left(\frac{\partial T}{\partial \dot{a}_1}\right) - \frac{\partial T}{\partial a_1} + \frac{\partial V}{\partial a_1} &= 0 \\ \cdot \quad \cdot \quad \cdot \quad \cdot \quad \cdot & \end{aligned}\right\} \tag{9}$$

In the application of Lagrange's equation (eqs. (9)), great simplification is obtained if the chosen modes are the natural modes of the uncoupled components; the rest of this paper is based on this choice. Equations (7) and (8) are then substituted into equations (9) to obtain the differential equations for free vibration. The characteristic equations for free vibrations are found by considering harmonic motion, that is,

$$\left.\begin{aligned} a_0 &= \tilde{a}_0 \sin \omega t \\ a_1 &= \tilde{a}_1 \sin \omega t \\ &\cdots\cdots \end{aligned}\right\} \tag{10}$$

where the amplitudes of a_0, a_1, . . . are denoted by $\tilde{a}_0$, $\tilde{a}_1$, ... The result of substituting equations (7) and (8) into equations (9) and making use of equations (10) leads to the characteristic equations which are given in matrix form as follows:

$$\begin{bmatrix}
M_F + M_e + pM_F + qM_R & M_e\frac{l_e}{l} + qM_2 + M_F\frac{l_{cg}}{l} & A_0 & B_0 & M_e y_1(l_e) + pM_F y_1(0) + qM_R y_1(l) & A_1 & B_1 & M_e \\
M_e\frac{l_e}{l} + qM_R + M_F\frac{l_{cg}}{l} & M_F\left(\frac{k}{l}\right)^2 + M_e\left(\frac{l_e}{l}\right)^2 + qM_R & 0 & B_0 & M_e\frac{l_e}{l}y_1(l_e) + qM_R y_1(l) & 0 & B_1 & M_e\frac{l_e}{l} \\
A_0 & 0 & C_0\left[1-\left(\frac{\Omega}{\omega}\right)^2\right] & 0 & y_1(0)A_0 & 0 & 0 & 0 \\
B_0 & B_0 & 0 & D_0\left[1-\left(\frac{\Omega}{\omega}\right)^2\right] & y_1(l)B_0 & 0 & 0 & 0 \\
pM_F y_1(0) + qM_R y_1(l) + M_e y_1(l_e) & M_e\frac{l_e}{l}y_1(l_e) + qM_R y_1(l) & y_1(0)A_0 & y_1(l)B_0 & \left[1-\left(\frac{\omega_{F,1}}{\omega}\right)^2\right]M_{F,1} + M_e y_1^2(l_e) + pM_F y_1^2(0) + qM_R y_1^2(l) & y_1(0)A_1 & y_1(l)B_1 & M_e y_1(l_e) \\
A_1 & 0 & 0 & 0 & y_1(0)A_1 & C_1\left[1-\left(\frac{\omega_{F,1}}{\omega}\right)^2 - K_{F,1}\left(\frac{\Omega}{\omega}\right)^2\right] & 0 & 0 \\
B_1 & B_1 & 0 & 0 & y_1(l)B_1 & 0 & D_1\left[1-\left(\frac{\omega_{R,1}}{\omega}\right)^2 - K_{R,1}\left(\frac{\Omega}{\omega}\right)^2\right] & 0 \\
M_e & M_e\frac{l_e}{l} & 0 & 0 & M_e y_1(l_e) & 0 & C & M_e\left[1-\left(\frac{\omega_e}{\omega}\right)^2\right]
\end{bmatrix}
\begin{Bmatrix} \tilde{b}_0 \\ \tilde{b}_0 \\ \tilde{a}_0 \\ \tilde{a}_0 \\ \tilde{b}_1 \\ \tilde{a}_1 \\ \tilde{a}_1 \\ \tilde{a}_f \end{Bmatrix} = 0 \tag{11}$$

where

$$A_0 = \frac{p}{R_F} \int_0^{R_F} m_F r_F \, dr_F \qquad B_0 = \frac{q}{R_R} \int_0^{R_R} m_R r_R \, dr_R$$

$$A_1 = p \int_0^{R_F} m_F x_1 \, dr_F \qquad B_1 = q \int_0^{R_R} m_R z_1 \, dr_R$$

$$C_0 = \frac{p}{R_F^2} \int_0^{R_F} m_F r_F^2 dr_F \qquad D_0 = \frac{q}{R_R^2} \int_0^{R_R} m_R r_R^2 dr_R$$

$$C_1 = p \int_0^{R_F} m_F x_1^2 dr_F \qquad D_1 = q \int_0^{R_R} m_R z_1^2 dr_R$$

$$K_{F,1} = \frac{p}{C_1} \int_0^{R_F} \bar{T}_F (x_1')^2 dr_F \qquad K_{R,1} = \frac{q}{D_1} \int_0^{R_R} \bar{T}_R (z_1')^2 dr_R$$

$$M_{f,1} = \int_0^{l} m_f y_1^2 ds \qquad \omega_e^2 = \frac{K_e}{M_e}$$

In the abbreviated notation used in the appendix, equation (11) can be written as

$$\left[H \right] \left\{ \eta \right\} = 0 \tag{11a}$$

Coupled Frequencies and Mode Shapes

The values of ω, the natural frequencies of the coupled modes of the helicopter, are determined by setting the determinant of equation (11) equal to zero. The coupled mode shapes are determined by substitution of the modal coefficients $\tilde{b}_0$, $\tilde{\tilde{b}}_0$, and so forth, obtained from equation (11), into equations (3) to (6).

Inspection of equation (11) reveals that, although there are eight degrees of freedom, the frequency term ω appears in only six of the diagonal terms when $\Omega \neq 0$ and in only four of the diagonal terms when $\Omega = 0$. Thus, the amount of work involved in the solution of the determinant can be reduced by changing the order of the matrix from eight to six when $\Omega \neq 0$ and from eight to four when $\Omega = 0$. The steps involved in this transformation as well as the final matrices obtained for $\Omega = 30$ radians per second and $\Omega = 0$ for the basic configuration are given in the appendix. The appendix also contains some pertinent remarks regarding methods for obtaining the modal coefficients.

Equations for Response of Helicopter to Applied Loads

Once the natural frequencies and shapes of the coupled modes are obtained, the next objective is to determine the response of the helicopter to applied aerodynamic loads. The calculation of the response necessitates a consideration of the damping of the structure. In the analysis that follows, a method is presented which permits the coupled mode shapes and frequencies determined by the methods presented in previous sections of this paper to be utilized, with the inclusion of structural damping, in the determination of the response of the helicopter to arbitrary forces.

If $\phi(\sigma,t)$ be designated as the deflection of the helicopter at station σ at time t (fig. 1), the differential equation of motion for an element of the helicopter at station σ is

$$(1 + ig_h)\frac{\partial^2}{\partial\sigma^2}\left(EI\frac{\partial^2\phi}{\partial\sigma^2}\right) + m\ddot{\phi} = F(\sigma,t) \tag{12}$$

where F is the applied force, g_h is the conventional structural damping coefficient, and simple harmonic motion is implied. If it is assumed that the total deflection can be expressed as a superposition of the natural coupled modes of the structure, then

$$\phi(\sigma,t) = \sum_{r=1}^{r=n} \alpha_r(t)\phi_r(\sigma) \tag{13}$$

where $\phi_r(\sigma)$ is the rth-coupled-mode shape and $\alpha_r(t)$ is the time-dependent coefficient of the rth mode. Substitution of equation (13) into equation (12) yields

$$\left(1 + ig_h\right)\alpha_1(t)\frac{\partial^2}{\partial\sigma^2}\left(EI\,\frac{\partial^2\phi_1}{\partial\sigma^2}\right) + \left(1 + ig_h\right)\alpha_2(t)\frac{\partial^2}{\partial\sigma^2}\left(EI\,\frac{\partial^2\phi_2}{\partial\sigma^2}\right) + \cdots + \left(1 + ig_h\right)\alpha_n(t)\frac{\partial^2}{\partial\sigma^2}\left(EI\,\frac{\partial^2\phi_n}{\partial\sigma^2}\right) =$$

$$-\ddot{\alpha}_1(t)m\phi_1 - \ddot{\alpha}_2(t)m\phi_2 - \cdots - \ddot{\alpha}_n(t)m\phi_n + F(\sigma,t) \tag{14}$$

Since the natural modes of vibration are defined by

$$\frac{\partial^2}{\partial\sigma^2}\left(EI\,\frac{\partial^2\phi_r}{\partial\sigma^2}\right) = \omega_r^2 m\phi_r \tag{15}$$

equation (14) can be written as

$$\left(1 + ig_h\right)\alpha_1(t)\omega_1^2 m\phi_1 + \left(1 + ig_h\right)\alpha_2(t)\omega_2^2 m\phi_2 + \cdots + \left(1 + ig_h\right)\alpha_n(t)\omega_n^2 m\phi_n =$$

$$-\ddot{\alpha}_1(t)m\phi_1 - \ddot{\alpha}_2(t)m\phi_2 - \cdots - \ddot{\alpha}_n(t)m\phi_n + F(\sigma,t) \tag{16}$$

Upon multiplication of equation (16) by ϕ_r, integrating over the length, and observing the conditions of orthogonality for natural modes, namely,

$$\left.\begin{aligned} \int_0^L m\phi_r\phi_s\,d\sigma &= 0 \qquad (r \neq s) \\ \int_0^L m\phi_r\phi_s\,d\sigma &= M_r \qquad (r = s) \end{aligned}\right\} \tag{17}$$

equation (16) becomes

$$\left(1 + ig_h\right)\alpha_r\omega_r^2 M_r = -\ddot{\alpha}_r M_r + \int_0^L F(\sigma,t)\phi_r\,d\sigma \tag{18}$$

In general, F will be a distributed force and, if necessary, the integral term of equation (18) can be evaluated. For purposes of illustration, however, it is assumed that F is a concentrated force and the rest

of the analysis is based on that assumption. The integral term of equation (18) is

$$\int_0^L F(\sigma,t)\phi_r \, d\sigma = F\phi_r(\sigma_A) \tag{19}$$

where F is the force applied and $\phi_r(\sigma_A)$ is the deflection of the rth mode at the point of application of the force. Therefore,

$$\left(1 + ig_h\right)\alpha_r\omega_r^2 M_r + \ddot{\alpha}_r M_r = F\phi_r(\sigma_A) \tag{20}$$

If α_r and F are expressed as the real parts of $\alpha_{r,0}e^{i\omega t}$ and $F_0e^{i\omega t}$, respectively, then

$$\left(1 + ig_h\right)\alpha_{r,0}\omega_r^2 M_r - \omega^2\alpha_{r,0}M_r = F_0\phi_r(\sigma_A) \tag{21}$$

The amplitude of α_r is

$$\alpha_{r,0} = \frac{\dfrac{F_0\phi_r(\sigma_A)}{\omega_r^2 M_r}}{\left[1 - \left(\dfrac{\omega}{\omega_r}\right)^2\right] + ig_h} \tag{22}$$

and, by definition, the coefficient of the motion in the rth mode is given by the real part of the following expression:

$$\alpha_r = \frac{\dfrac{F_0\phi_r(\sigma_A)}{\omega_r^2 M_r}}{\left[1 - \left(\dfrac{\omega}{\omega_r}\right)^2\right] + ig_h} e^{i\omega t} = \left(P_r - iQ_r\right)e^{i\omega t} \tag{23}$$

where

$$\left.\begin{aligned} P_r &= \frac{\dfrac{F_0\phi_r(\sigma_A)}{\omega_r^2 M_r}}{\left[1 - \left(\dfrac{\omega}{\omega_r}\right)^2\right]^2 + g_h^2}\left[1 - \left(\frac{\omega}{\omega_r}\right)^2\right] \\ Q_r &= \frac{\dfrac{F_0\phi_r(\sigma_A)}{\omega_r^2 M_r}}{\left[1 - \left(\dfrac{\omega}{\omega_r}\right)^2\right]^2 + g_h^2}\, g_h \end{aligned}\right\} \tag{24}$$

Substitution of equation (23) into equation (13) yields the total response ϕ

$$\phi(\sigma,t) = \left[\sum_{r=1}^{r=n}\left(P_r - iQ_r\right)\phi_r\right]e^{i\omega t} \tag{25}$$

the amplitude of which is

$$|\phi| = \sqrt{\left(\sum_{r=1}^{r=n} P_r\phi_r\right)^2 + \left(\sum_{r=1}^{r=n} Q_r\phi_r\right)^2} = \sqrt{X^2 + Y^2} \tag{26}$$

Then $|\phi|$ is the amplitude of vibration at any station σ in response to a harmonic force, applied at $\sigma = \sigma_A$, which has an amplitude F_0 and a frequency ω. It should be noted in the application of equation (26) that $\phi_1, \phi_2, \ldots \phi_n$ are the values of the coupled modes at station σ.

In the event that it is desired that the response at any station be calculated for loads applied at several different stations, then some reduction of the work required may be obtained by suitably modifying the coefficients P_r and Q_r. Assume, for example, that $(P_r)_I$ and $(Q_r)_I$ are the in-phase and out-of-phase components of the response in the rth mode to an oscillating load applied at the front hub and designated by

subscript I. From equation (26), the response in the rth mode at the same station to a load of the same magnitude applied in the same direction at the rear hub, and designated by subscript II, is given by the components:

$$\left.\begin{aligned}(P_r)_{II} &= (P_r)_I \phi_r(\sigma_A)_{II} \Big/ \phi_r(\sigma_A)_I \\ (Q_r)_{II} &= (Q_r)_I \phi_r(\sigma_A)_{II} \Big/ \phi_r(\sigma_A)_I\end{aligned}\right\} \tag{27}$$

The in-phase and out-of-phase components of the response due to all the modes is then given by

$$\left.\begin{aligned}X_{II} &= \sum_{r=1}^{r=n} (P_r)_{II} \phi_r \\ Y_{II} &= \sum_{r=1}^{r=n} (Q_r)_{II} \phi_r\end{aligned}\right\} \tag{28}$$

The response due to any combination of forces applied at either or both hubs in the same or opposite directions is then obtained by adding X_I, X_{II}, Y_I, and Y_{II} in the proper sense and proportions.

DISCUSSION OF RESULTS

Calculation of Coupled Frequencies and Mode Shapes

Scope of the calculations.- The analysis derived in this paper was used to calculate the natural coupled frequencies of a tandem helicopter having the structural parameters given in table I. The resulting modal coefficients are given in table II and the natural frequencies and mode shapes are given in figures 2 and 3. Some additional calculations were made to evaluate the effects of the natural frequency of the uncoupled fuselage system and the Southwell coefficient of the blades on the natural frequencies of the coupled system. These results are shown in figures 4 and 5. Calculations were also made for a three-degree-of-freedom system

(bending of the fuselage and bending of the blades on the front and rear rotors) and the resulting frequencies are compared with appropriate frequencies for the eight-degree-of-freedom system in figure 6 to obtain some idea of the relative contributions of the various degrees of freedom to the overall problem.

Frequencies and mode shapes for the basic configuration.- The basic configuration is designated by the parameters given in table I which correspond closely to those of an existing tandem helicopter. The natural frequencies and mode shapes of the coupled system were calculated for this configuration for three rotor speeds: namely, 0, 20, and 30 radians per second. The natural frequencies are plotted in figure 2 as a function of rotor speed, and the modal coefficients are tabulated in table II for each of the six natural frequencies and for each of the three rotor speeds. A rotor speed of 30 radians per second corresponds very closely to the normal operating rotor speed for the chosen helicopter. The modal coefficients presented in table II for this speed were used in equations (3) to (6) to obtain the mode shapes which are presented in figure 3 and which are also sketched in figures 2, 4, and 5 to identify the modes of vibration that correspond to the different natural frequencies of the coupled system.

The effect of coupling of the various degrees of freedom on the natural frequencies is indicated in figure 2 by a comparison of the coupled frequencies (shown by solid lines) with the uncoupled frequencies (shown by short-dashed lines). The curve for uncoupled blade first bending represents the blades of both the front and rear rotors. There are also short-dashed curves for uncoupled blade flapping; however, these curves cannot be seen inasmuch as they are coincident with the frequency curve for the lower coupled mode. The frequencies of the two- and three-per-revolution harmonic component of the aerodynamic loading (designated 2-P and 3-P herein and indicated by the long-dashed lines in fig. 2) are also presented to permit comparison with the natural frequencies. With the exception of the engine translational frequency and the fuselage first-bending frequency, the differences between the coupled and uncoupled frequencies are negligible at low rotor speeds. As the rotor speed is increased, the uncoupled frequencies of the fuselage mode and the blade bending modes approach each other, and, as expected, the effects of coupling become pronounced.

The helicopter used as an example for these calculations has three blades on each rotor, and, therefore, the 3-P components of the aerodynamic loading on the rotor blades are additive at the respective hubs. Thus, the region of primary importance on the frequency diagram of figure 2 is the region at or near the crosshatched marks on the 3-P line which brackets the normal variation of the design rotor speed.

Inasmuch as the two rotors rotate in opposite directions with a phase difference of blade position on the two rotors of approximately 60°, blades from both rotors are advancing into the wind simultaneously three times per revolution of each rotor. This condition suggests that the resultant 3-P periodic forces at the two hubs are in phase and would be particularly effective in the excitation of the symmetrical modes of the helicopter which have natural frequencies in the general region of 85 radians per second. Figure 2 shows that there are three coupled modes of the helicopter which have natural frequencies reasonably close to the 3-P frequency, two of which are symmetrical and the other antisymmetrical. In view of the preceding discussion, the data of figure 2 indicate that at the higher rotor speed (30 radians per second) the response of this helicopter in the third symmetrical mode to the 3-P oscillating excitation forces would be increased substantially by resonance amplification. Furthermore, if there is a component of the 3-P aerodynamic loading at the two rotor hubs which is out of phase, it appears likely that the structural response in the second antisymmetrical mode would also be increased by resonance amplification.

The mode shapes presented in figure 3 show that the mode shapes alternate between symmetrical and antisymmetrical configurations. The relative motion of the engine with respect to the fuselage is shown to be negligible for the lower frequency modes but becomes relatively large at the highest frequency mode (sixth-coupled-mode shape).

Effect of Variations in Uncoupled Components

Effect of natural uncoupled frequency of the fuselage.- The analysis presented in this paper permits the inclusion of the natural uncoupled frequency of the fuselage as one of the parameters. This frequency can be calculated by analytical methods such as those of references 1 and 2; however, this requires an accurate knowledge of the mass and stiffness distribution of the fuselage which may be difficult to obtain. The accuracy to which this frequency can be obtained experimentally for a given helicopter depends upon such considerations as the manner of support and the type of shaker installation. Since this frequency is one of the primary parameters, it is of interest to determine to what extent the natural frequencies of the coupled modes are changed by variations of the uncoupled frequency of the fuselage. Conversely, if the natural frequencies of the coupled system for a known design value of the natural uncoupled frequency of the fuselage are of such a magnitude as to lead to resonance amplification of the structural response, it is desirable to evaluate the extent to which the coupled frequencies can be changed by varying the uncoupled frequency of the fuselage.

An indication of the change in the natural frequencies of the coupled modes due to changes in the uncoupled frequency of the fuselage is shown by the curves of figure 4. The calculations show that the frequencies of

the second and third symmetrical modes are changed appreciably whereas the frequencies of the antisymmetrical modes are not affected. Since the amount of fuselage bending in the antisymmetrical modes is negligible in comparison with the amount of fuselage bending in the symmetrical modes, the results shown in figure 4 are in agreement with expectations.

Effect of Southwell coefficient for the blade first elastic flapwise bending mode.- The value of the Southwell coefficient chosen for the blade first elastic flapwise bending mode has a direct effect on the uncoupled frequency of the rotating blade. An indication of the effect of this parameter on the coupled frequencies is shown in figure 5. The value of $K_{F,1}$ estimated by means of reference 4 for the blade considered is 6.2 and the range of values chosen for these calculations is believed to be more than adequate to allow for estimation errors. These calculations show that the coupled frequencies of both the symmetrical and antisymmetrical modes which have frequencies approximately equal to the uncoupled blade-bending frequencies are increased slightly as the Southwell coefficient is increased, and that errors in the values of the coupled frequencies due to the estimation of the Southwell coefficient $K_{F,1}$ should not exceed 2 or 3 percent.

Comparison of Results of Three-Mode and Eight-Mode Analysis

Figure 2 shows that the uncoupled modes which are primarily affected by coupling in the frequency region of the 3-P excitation forces are fuselage bending and the bending of the blades on the front and rear rotors. Calculations were made to determine how well the frequencies of the coupled modes could be predicted by using only these three uncoupled modes. The calculation procedure consisted of retaining only the fifth, sixth, and seventh rows and columns of the frequency determinant of equation (11). The results are given in figure 6 together with the corresponding frequencies obtained from the eight-mode analysis. A comparison of the frequencies for the two cases shows that the frequencies calculated by the three-mode analysis are from 3 to 6 percent lower than those obtained by the eight-mode analysis, and suggests that a three-mode analysis might be useful for obtaining a first approximation of the coupled frequencies in this region for configurations similar to the one treated herein.

Calculation of the Response of the Helicopter to Applied Loads

The methods developed in the previous sections of this paper were applied to calculate the amplitudes of the response of the helicopter at the location of the cockpit for harmonic oscillating forces applied at the front and rear rotor hubs. The amplitudes of vibration were calculated as a function of frequency of the periodic force for one value

of damping ($g_h = 0.1$) and at a rotor speed of 30 radians per second for the four cases which follow:

Case I: Oscillating force of unit magnitude applied in a vertical direction at the front rotor hub.

Case II: Oscillating force of unit magnitude applied in a vertical direction at the rear rotor hub.

Case III: Oscillating force of one-half unit magnitude applied in a vertical direction at both the front and rear rotor hubs in the same direction.

Case IV: Oscillating force of one-half unit magnitude applied in a vertical direction at the front and rear rotor hubs in opposite directions (producing a pure pitching moment on the fuselage).

The in-phase and out-of-phase components of the response, or cockpit deflections, are given in figures 7 and 8 as a function of frequency for cases I and II, respectively. The natural coupled frequencies are indicated by the vertical dashed lines at the bottom of the figures. The response curves are presented to familiarize the reader with the nature of the components and as an aid in the calculation of the cockpit deflections due to other combinations of loads at the front and rear rotor hubs. The cockpit deflections for cases III and IV as well as for cases I and II were obtained by suitably combining the in-phase and out-of-phase components of figures 7 and 8 as outlined in the analysis section.

The amplitude of the cockpit vibrations resulting from the oscillating forces applied to the hub in the four cases previously outlined are given in figures 9 to 12, respectively. Before discussing these figures, the reader's attention is again directed to figure 2 where, at the rotor speed of 30 radians per second for which these response calculations are appropriate, six distinct natural frequencies are indicated within the range from 0 to 180 radians per second. These natural frequencies are indicated by the vertical dashed lines at the bottom of figures 9 to 12. For the hypothetical case of zero damping, it is expected then that the response curves similar to those of figures 9 to 12 would indicate six peaks of infinite amplitude at frequencies corresponding to the natural frequencies. With the inclusion of a small amount of damping, these peaks become finite and as the damping is progressively increased some of the peaks disappear. The peaks which remain when the forces are applied in a given manner indicate the modes in which the given forces are more effective in doing work.

The curves of figures 9 to 12 show the responses obtained for $g_h = 0.1$ for the four cases investigated. The manner of application of the load in

each case is indicated in the figure by the accompanying sketch of a tandem helicopter. In a few instances where the number of calculated points, indicated by the small circles, are insufficient to define the peaks completely, the peaks are indicated by the long-dashed lines. All the figures indicate peaks at frequencies of approximately 32, 72, and 92 radians per second and show that the coupled modes which contribute most to the responses are the second, third, and fifth coupled modes, respectively, of figure 3. This effect was also observed during the calculations by inspection of the values of the individual values of P_r and Q_r. (See eq. (24)). The most significant deviation from the general trend of high responses at forcing frequencies near the natural frequencies of the aforementioned coupled modes is found in figure 12. In this case, the response to forces applied so as to produce a moment on the helicopter is found to diminish considerably at the higher forcing frequencies. This reduction of the response at the higher frequencies appears significant because it indicates that, if the aerodynamic forcing functions which are usually encountered in flight could be forced to occur in an antisymmetric manner, the response at a frequency of 3-P or 90 radians per second would be substantially reduced over that obtained for symmetrically applied loadings as shown by figure 11.

Perhaps one of the most significant points brought out by these studies is the fact that it is not always possible to obtain the natural frequencies of all the coupled modes of a structure by observing the response of the structure to arbitrary inputs. Conversely, if the applied loads are realistically chosen to be representative of those encountered under normal flight conditions, the peaks of the response curve appear to give fairly good indications of the natural frequencies of the more important coupled modes.

Considerations Regarding Further Refinement of the Method

The studies presented in this paper - although believed to be useful in the evaluation and reduction of the critical vibrations of tandem helicopters by emphasizing the importance of coupled natural frequencies and mode shapes, providing a method for estimating them, and, in turn, using them to determine the response of the helicopter to applied loads - do not provide a complete answer to the problem. For one thing, the number of degrees of freedom treated, although they are believed to be the more important ones, are not nearly sufficient to predict all the coupled frequencies. A more complete analysis would also include the fore-and-aft motions of the front and rear rotor hubs, the pitching motions of the engine, and the chordwise motions of the blades in bending and rotation about the drag hinge. In fact, each blade should be treated as an independent flexible structure, subject only to the boundary conditions imposed by the vibrating hub to which it is attached. The complexities

of treating such a system analytically are apparent and they exceed the intent of the present paper.

The method of analysis presented in this paper for the longitudinal vibrations - namely, the coupling of the structural properties of the uncoupled components of the helicopter to obtain the natural frequencies, mode shapes, and response of the coupled system - also appears applicable to the treatment of the case of coupled side bending and torsion of the fuselage. Vibrations of this type have been observed in tandem helicopters and a study of the effects of the significant parameters involved would provide useful design information.

CONCLUDING REMARKS

A method is presented for the calculation of the coupled frequencies and mode shapes of vibrations in the longitudinal plane of symmetry of tandem helicopters. The coupled frequencies and mode shapes are then used to calculate the response of the helicopter to applied loads. Sample calculations were made for an existing helicopter and these calculations yield the coupled frequencies and mode shapes and the deflection of the cockpit to oscillating loads applied at the front and rear rotor hubs. The mode shapes, both symmetrical and antisymmetrical, show the relative deflections of the various components of the structure when excited in a given mode.

The results of the calculations for the helicopter chosen show that the natural frequencies for the coupled modes may differ considerably from the natural frequencies for the uncoupled modes; therefore, there may be a need for making a rather comprehensive coupled-mode analysis so that regions of adverse dynamic response can be detected and avoided.

The results of calculations for different values of the uncoupled natural frequency of the fuselage indicate that the natural frequencies of the symmetrical coupled modes in the general range of the uncoupled frequency of the fuselage vary appreciably with changes in the uncoupled frequency of the fuselage; however, the effect on the natural frequency of the antisymmetrical coupled modes is negligible. An increase in the values of the Southwell coefficient for the blade first elastic flapwise bending mode resulted in a small increase in the coupled frequencies of both the antisymmetrical and symmetrical coupled modes having frequencies in the proximity of the blade frequencies.

The response calculations show that the amplitude of the vertical vibrations of the cockpit changes appreciably with changes in frequency, point of application, and manner of application of applied oscillating forces. High amplitudes occur when the frequencies of the applied oscillating forces are approximately equal to the natural frequencies of the second, third, and fifth coupled modes of the helicopter and the results

of calculations indicate that the contributions of other modes to the vibrations of the cockpit are secondary for the specific forces chosen. The results indicate that the vibration of the cockpit due to oscillating forces having a frequency of 3 per revolution (3-P) or 90 radians per second are substantially greater for forces applied symmetrically at the front and rear rotor hubs than for forces applied antisymmetrically. The results also emphasize that it is very unlikely that all natural frequencies of a helicopter could be obtained by observing the response of the helicopter to oscillating forces applied at any given point.

Langley Aeronautical Laboratory,
National Advisory Committee for Aeronautics,
Langley Field, Va., August 2, 1956.

APPENDIX

STEPS IN REDUCING THE ORDER OF THE MATRIX EQUATION

Procedure When $\Omega \neq 0$

When $\Omega \neq 0$, the matrix of the differential equations of motion, equation (11) of the text, can be written in concise notation of submatrices as follows:

$$\begin{bmatrix} H \end{bmatrix} \begin{Bmatrix} \eta \end{Bmatrix} = \begin{bmatrix} [\alpha] & [\beta] \\ [\beta]' & [\delta] \end{bmatrix} \begin{Bmatrix} \{\eta_1\} \\ \{\eta_2\} \end{Bmatrix} - \frac{1}{\omega^2} \begin{bmatrix} 0 & 0 \\ 0 & [\epsilon] \end{bmatrix} \begin{Bmatrix} \{\eta_1\} \\ \{\eta_2\} \end{Bmatrix} = 0 \tag{A1}$$

where

$$[\alpha] = \begin{bmatrix} M_f + M_e + pM_F + qM_R & M_e \frac{l_e}{l} + qM_R + M_f \frac{l_{cg}}{l} \\ M_e \frac{l_e}{l} + qM_R + M_f \frac{l_{cg}}{l} & M_f\left(\frac{k}{l}\right)^2 + M_e\left(\frac{l_e}{l}\right)^2 + qM_R \end{bmatrix} \tag{A2}$$

$$[\beta] = \begin{bmatrix} A_0 & B_0 & M_e y_1(l_e) + pM_F y_1(0) + qM_R y_1(l) & A_1 & B_1 & M_e \\ 0 & B_0 & M_e \frac{l_e}{l} y_1(l_e) + qM_R y_1(l) & 0 & B_1 & M_e \frac{l_e}{l} \end{bmatrix} \tag{A3}$$

$$\left[\beta\right]' = \text{Transpose of } \left[\beta\right] \tag{A4}$$

$$\left[\delta\right] = \begin{bmatrix} C_0 & 0 & y_1(0)A_0 & 0 & 0 & 0 \\ 0 & D_0 & y_1(l)B_0 & 0 & 0 & 0 \\ y_1(0)A_0 & y_1(l)B_0 & M_{f,1} + M_e y_1^2(l_e) + pM_F y_1^2(0) + qM_R y_1^2(l) & y_1(0)A_1 & y_1(l)B_1 & M_e y_1(l_e) \\ 0 & 0 & y_1(0)A_1 & C_1 & 0 & 0 \\ 0 & 0 & y_1(l)B_1 & 0 & D_1 & 0 \\ 0 & 0 & M_e y_1(l_e) & 0 & 0 & M_e \end{bmatrix} \tag{A5}$$

$$\left[\epsilon\right] = \begin{bmatrix} C_0\Omega^2 & & & & & \\ & D_0\Omega^2 & & & & \\ & & (\omega_{r,1})^2 M_{f,1} & & & \\ & & & C_1\left[(\omega_{F,1})^2 + K_{F,1}\Omega^2\right] & & \\ & & & & D_1\left[(\omega_{R,1})^2 + K_{R,1}\Omega^2\right] & \\ & & & & & M_e\omega_e^2 \end{bmatrix} \tag{A6}$$

$$\left\{\eta_1\right\} = \begin{Bmatrix} \tilde{b}_0 \\ \tilde{\tilde{b}}_0 \end{Bmatrix} \tag{A7}$$

and

$$\left\{\eta_2\right\} = \begin{Bmatrix} \tilde{a}_0 \\ \tilde{c}_0 \\ \tilde{b}_1 \\ \tilde{a}_1 \\ \tilde{c}_1 \\ \tilde{w}_f \end{Bmatrix} \tag{A8}$$

If $\left[\alpha\right] \equiv \alpha$, $\left\{\eta_1\right\} \equiv \eta_1$, and so forth, then the algebraic expressions for the matrix equation, equation (A1), are as follows:

$$\alpha\eta_1 + \beta\eta_2 = 0 \tag{A9}$$

$$\beta'\eta_1 + \delta\eta_2 = \frac{1}{\omega^2}\epsilon\eta_2 \tag{A10}$$

If equation (A9) is solved for η_1 and the result substituted into equation (A10), then

$$\left(\delta - \beta'\alpha^{-1}\beta\right)\eta_2 = \frac{1}{\omega^2}\epsilon\eta_2 \tag{A11}$$

Multiplication of equation (A11) by the inverse of ϵ reduces it to the desired form; however, the resulting matrix is unsymmetrical and poorly conditioned. These characteristics are undesirable if iteration procedures are used to determine the frequencies and mode shapes, particularly so in this case because the frequencies are in some instances nearly equal to each other. The condition of the matrix can be improved and the matrix can be made symmetrical by the following transformation:

$$\sqrt{\epsilon}\,\eta_2 = \xi \tag{A12}$$

which yields the final matrix

$$\left[\sqrt{\epsilon}^{-1}\left(\delta - \beta'\alpha^{-1}\beta\right)\sqrt{\epsilon}^{-1} - \frac{1}{\omega^2}\right]\xi = 0 \tag{A13}$$

The natural frequencies are then obtained when the determinant of equation (A13) vanishes. When the natural frequencies are substituted back into the matrix (eq. (A13)) and the value of unity assigned to one of the coefficients (for example, ξ_η), the rest of the coefficients ξ_1, ξ_2, and so forth, can be obtained. If an iteration procedure is used, the values of ξ are determined simultaneously with the natural frequencies. In either case, the mode shapes are then obtained as follows:

$$\eta_1 = -\alpha^{-1}\beta\,\sqrt{\epsilon}^{-1}\xi \tag{A14}$$

and

$$\eta_2 = \sqrt{\epsilon}^{-1}\xi \tag{A15}$$

The relative magnitudes of the elements of equation (A13) are illustrated by the following matrix which results when $\Omega = 30$ radians per second and the parameters are those for the basic configuration:

$$\begin{bmatrix} 0.0001715 - \frac{1}{\omega^2} & -0.00002270 & 0.00008273 & -0.0000194\!4 & 0.0001195 & -0.00002808 \\ -0.00002270 & 0.00004242 - \frac{1}{\omega^2} & -0.0000004435 & 0.0000001042 & -0.00003199 & 0.000007518 \\ 0.00008273 & -0.0000004435 & 0.001030 - \frac{1}{\omega^2} & 0.00001907 & 0.00002841 & -0.000006676 \\ -0.0000194\!4 & 0.0000001042 & 0.00001907 & 0.0001563 - \frac{1}{\omega^2} & -0.000006676 & 0.000001569 \\ 0.0001195 & -0.00003199 & 0.00002841 & -0.000006676 & 0.001039 - \frac{1}{\omega^2} & 0.00001684 \\ -0.00002808 & 0.000007518 & -0.000006676 & 0.000001569 & 0.00001684 & 0.0001568 - \frac{1}{\omega^2} \end{bmatrix} \begin{Bmatrix} \xi_1 \\ \xi_2 \\ \xi_3 \\ \xi_4 \\ \xi_5 \\ \xi_6 \end{Bmatrix} = 0 \tag{A16}$$

Procedure When $\Omega = 0$

When $\Omega = 0$, the frequency parameter $1/\omega^2$ occurs in only the last four rows and columns of equation (11). The transformation of the matrix for the solution in this case is accomplished in the same fashion as for $\Omega \neq 0$ except that the submatrices (α, β, β', δ, ϵ, η_1, and η_2 of eq. (A1)) are of the fourth order. The relative magnitudes of the elements of the final matrix for $\Omega = 0$ and for the basic parameters are shown by the following equation:

$$\begin{bmatrix} 0.0001516 - \frac{1}{\omega^2} & -0.00006283 & -0.00009185 & -0.00001905 \\ -0.00006283 & 0.001515 - \frac{1}{\omega^2} & 0.00001759 & -0.0000003405 \\ -0.00009185 & 0.00001759 & 0.001521 - \frac{1}{\omega^2} & 0.00002506 \\ -0.00001905 & -0.0000003405 & 0.00002506 & 0.00004143 - \frac{1}{\omega^2} \end{bmatrix} \begin{Bmatrix} \xi_1 \\ \xi_2 \\ \xi_3 \\ \xi_4 \end{Bmatrix} = 0 \qquad (A17)$$

REFERENCES

1. Houbolt, John C., and Anderson, Roger A.: Calculation of Uncoupled Modes and Frequencies in Bending or Torsion of Nonuniform Beams. NACA TN 1522, 1948.

2. Myklestad, N. O.: Vibration Analysis. McGraw-Hill Book Co., Inc., 1944, pp. 184-214.

3. Brooks, George W.: Analytical Determination of the Natural Coupled Frequencies of Tandem Helicopters. Jour. Am. Helicopter Soc., vol. 1, no. 3, July 1956, pp. 39-52.

4. Yntema, Robert T.: Simplified Procedures and Charts for the Rapid Estimation of Bending Frequencies of Rotating Beams. NACA TN 3459, 1955. (Supersedes NACA RM L54G02.)

TABLE I.- PARAMETERS USED IN CALCULATIONS

(a) Blade parameters (blades on front and rear rotor assumed to be identical)

[$\omega_{F,1} = \omega_{R,1} = 25.3$ radians/sec; $K_{F,1} = K_{R,1} = 6.2$; $R_F = R_R = 210$ in.; $p = q = 3$; $M_F = M_R = 0.194$ lb-sec^2/in.]

Station	Radial location, r_F or r_R, in.	Mass distribution, m_F or m_R, lb-sec^2/in.^{2}	First-bending mode shape, x_1 or z_1, in.
1	10.5	3.03	-0.09
2	31.5	1.52	-.27
3	52.5	.67	-.42
4	73.5	.59	-.50
5	94.5	.59	-.53
6	115.5	.53	-.50
7	136.5	.45	-.34
8	157.5	.40	-.07
9	178.5	.50	.28
10	199.5	.59	.75

(b) Fuselage and engine parameters

[$\omega_{f,1} = 89.2$ radians/sec; $\omega_e = 130$ radians/sec; $M_e = 2.861$ lb-sec^2/in.; $l_e/l = 0.735$]

Station	Fuselage location, s/l	Length of fuselage element, Δs, in.	Mass of fuselage element, $m_f \Delta s$, lb-sec^2/in.	First-bending mode shape, y_1, in.
1	0	32.44	1.28	0.76
2	.123	32.44	1.98	.36
3	.250	32.44	.42	.03
4	.375	32.44	.86	-.21
5	.500	32.44	2.12	-.36
6	.625	24.46	.80	-.38
7	.735	40.42	.23	-.27
8	.875	32.44	.81	.26
9	1.000	32.44	1.58	1.00

TABLE II.- MODAL COEFFICIENTS

	Modal coefficients for natural frequencies -					
	ω_1	ω_2	ω_3	ω_4	ω_5	ω_6
Ω = 0						
$\tilde{b}_0$	-------	------	-2.362	86.36	-0.02010	0.02635
$\tilde{\bar{b}}_0$	-------	------	-0.6313	-157.3	0.1598	-1.736
$\tilde{a}_0$	-------	------	2.652	-144.2	-1.224	-1.301
$\tilde{c}_0$	-------	------	3.299	115.7	-1.886	1.174
$\tilde{b}_1$	-------	------	1	1	1	1
$\tilde{a}_1$	-------	------	-182.1	2,802	1.043	1.032
$\tilde{c}_1$	-------	------	-226.5	-2,250	1.607	-0.9300
$\tilde{w}_f$	-------	------	-0.1233	-1.212	-0.1182	4.266
Ω = 20 radians/sec						
$\tilde{b}_0$	-3.925	123.1	-0.2716	32.21	-0.01219	0.03148
$\tilde{\bar{b}}_0$	-0.9383	-225.3	-0.04228	-56.51	0.1701	-1.748
$\tilde{a}_0$	153.4	-2,183	-0.9310	-62.22	-1.310	-1.330
$\tilde{c}_0$	187.5	1,782	-1.308	43.95	-2.028	1.204
$\tilde{b}_1$	1	1	1	1	1	1
$\tilde{a}_1$	0.6192	-26.11	-21.40	1,060	1.684	1.148
$\tilde{c}_1$	0.7558	21.31	-30.06	43.95	2.608	-1.040
$\tilde{w}_f$	-0.1227	-1.146	-0.1252	-2.282	-0.1171	4.273
Ω = 30 radians/sec						
$\tilde{b}_0$	-1.552	62.72	-0.07493	35.59	0.009242	0.04096
$\tilde{\bar{b}}_0$	-0.4512	-113.6	0.09865	-60.30	0.2010	-1.775
$\tilde{a}_0$	61.00	-1,123	-1.369	-69.86	-1.425	-1.366
$\tilde{c}_0$	77.30	881.8	-2.045	45.57	-2.242	1.266
$\tilde{b}_1$	1	1	1	1	1	1
$\tilde{a}_1$	0.1760	-15.41	-4.654	1,188	3.734	1.389
$\tilde{c}_1$	0.2225	12.11	-6.968	-776.4	5.883	-1.274
$\tilde{w}_f$	-0.1239	-1.312	-0.1223	-5.586	-0.1128	4.293

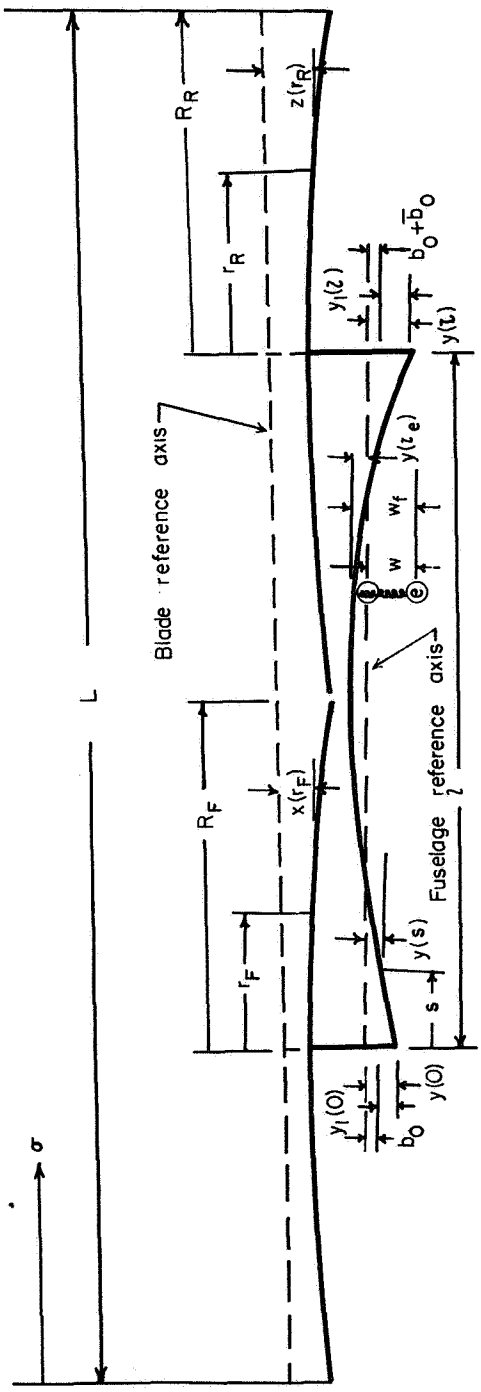

Figure 1.- Coordinates and displacements.

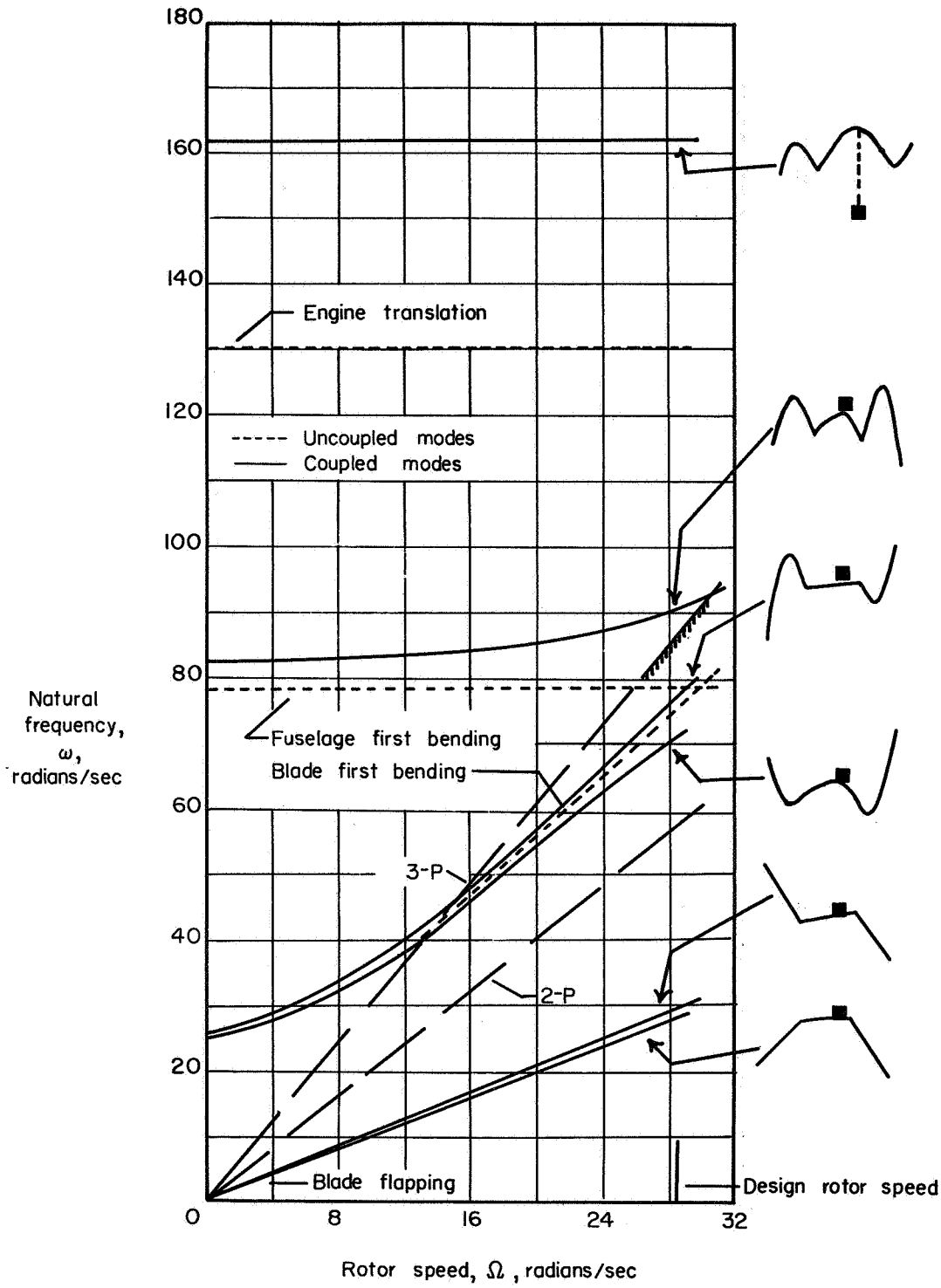

Figure 2.- Variation of natural frequencies with rotor speed.

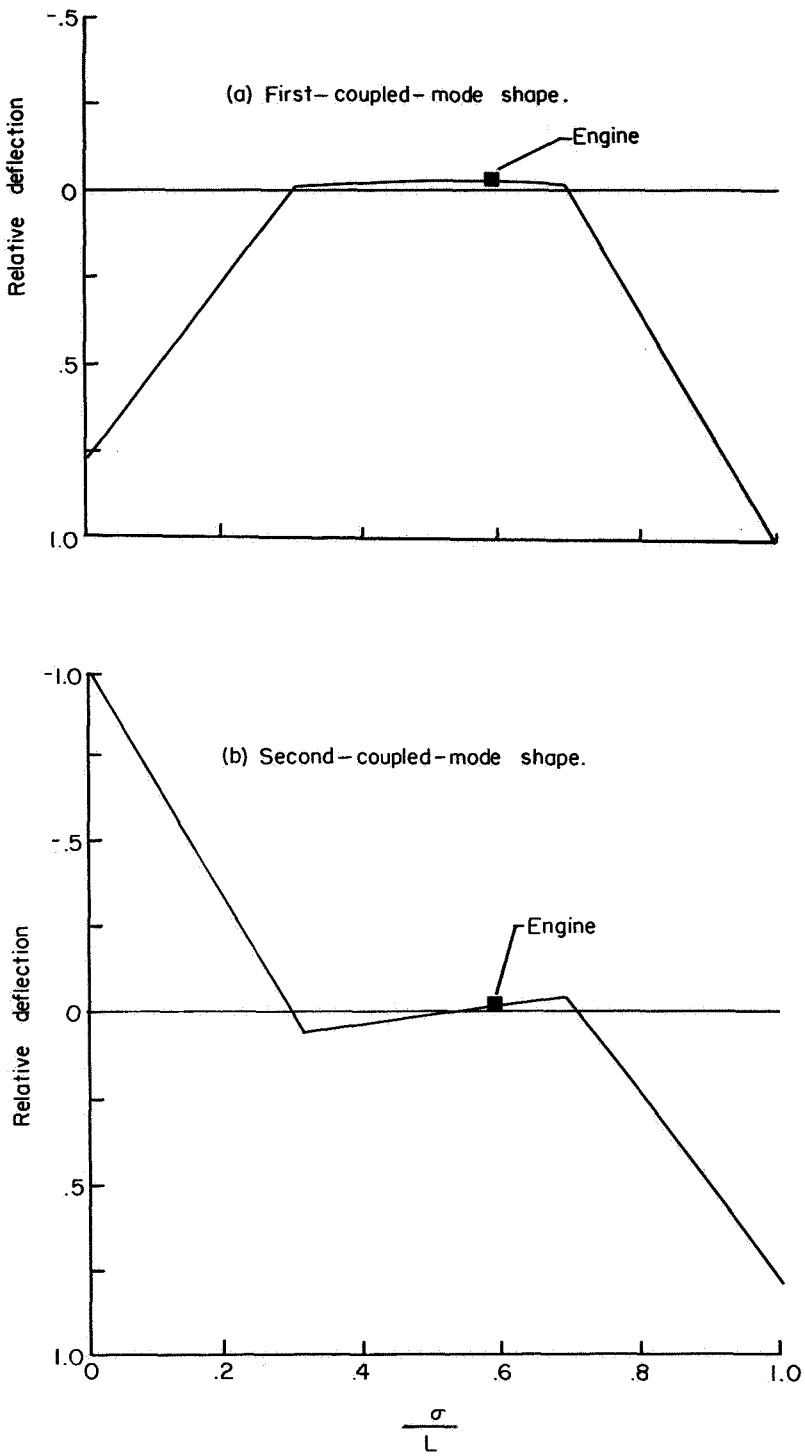

Figure 3.- Mode shapes of coupled rotor-fuselage system.

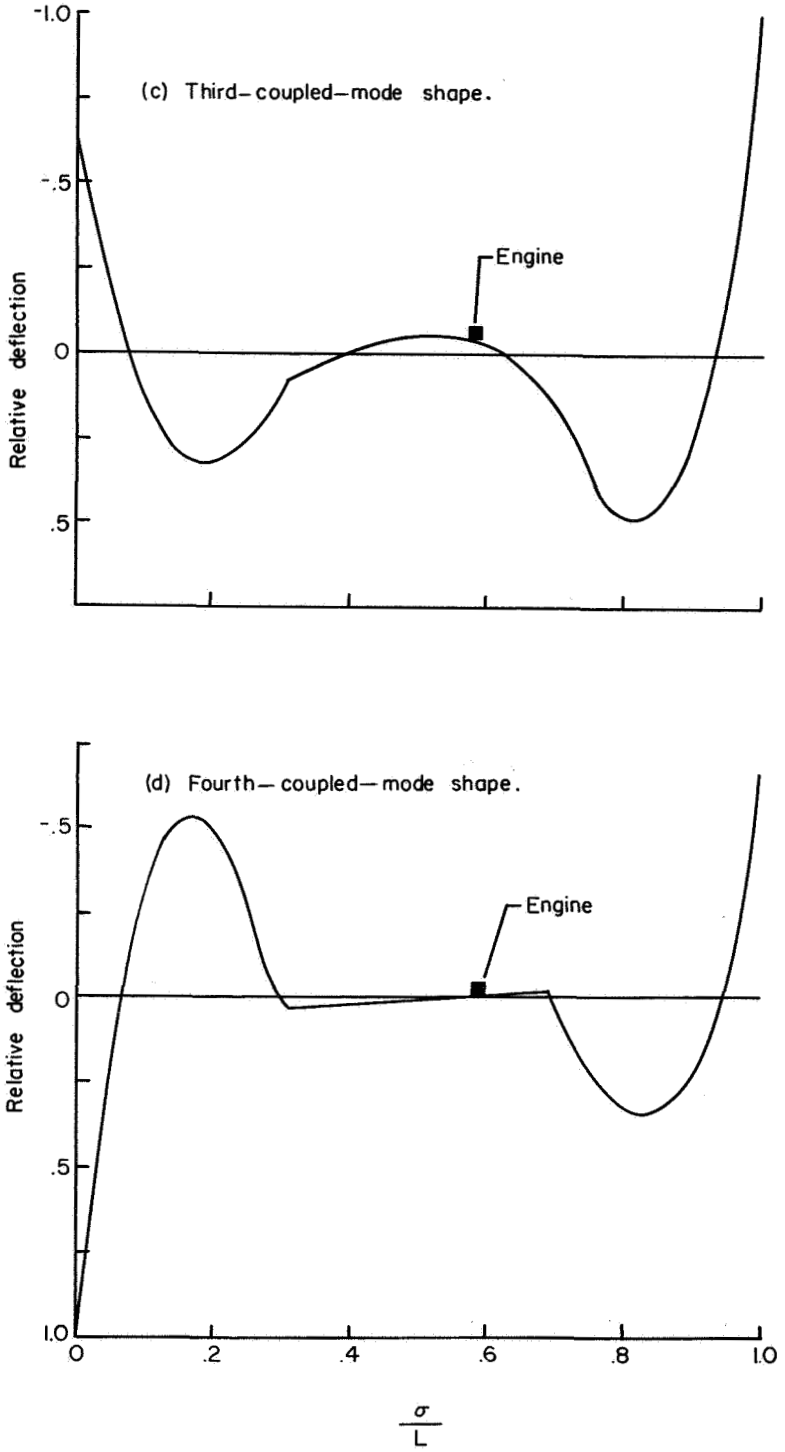

Figure 3.- Continued.

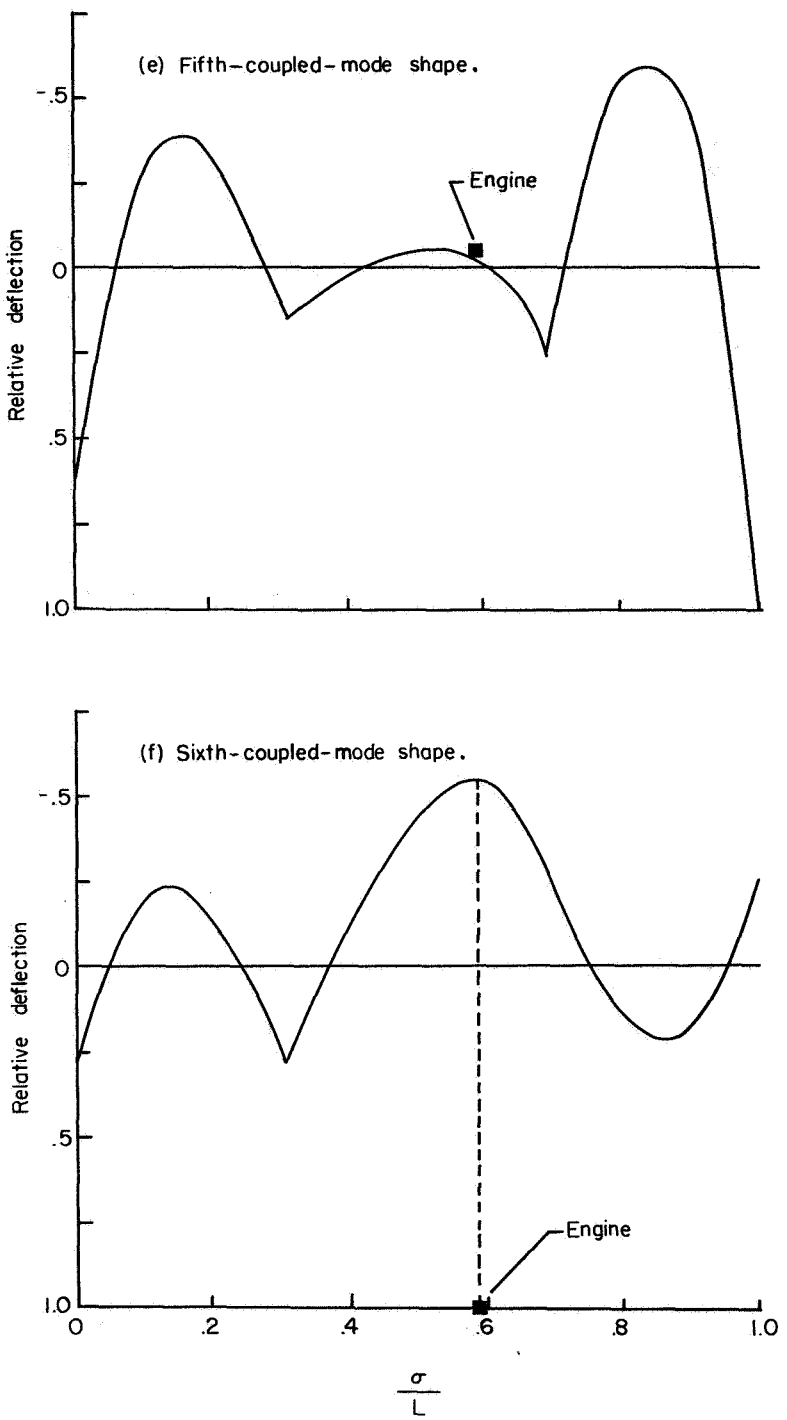

Figure 3.- Concluded.

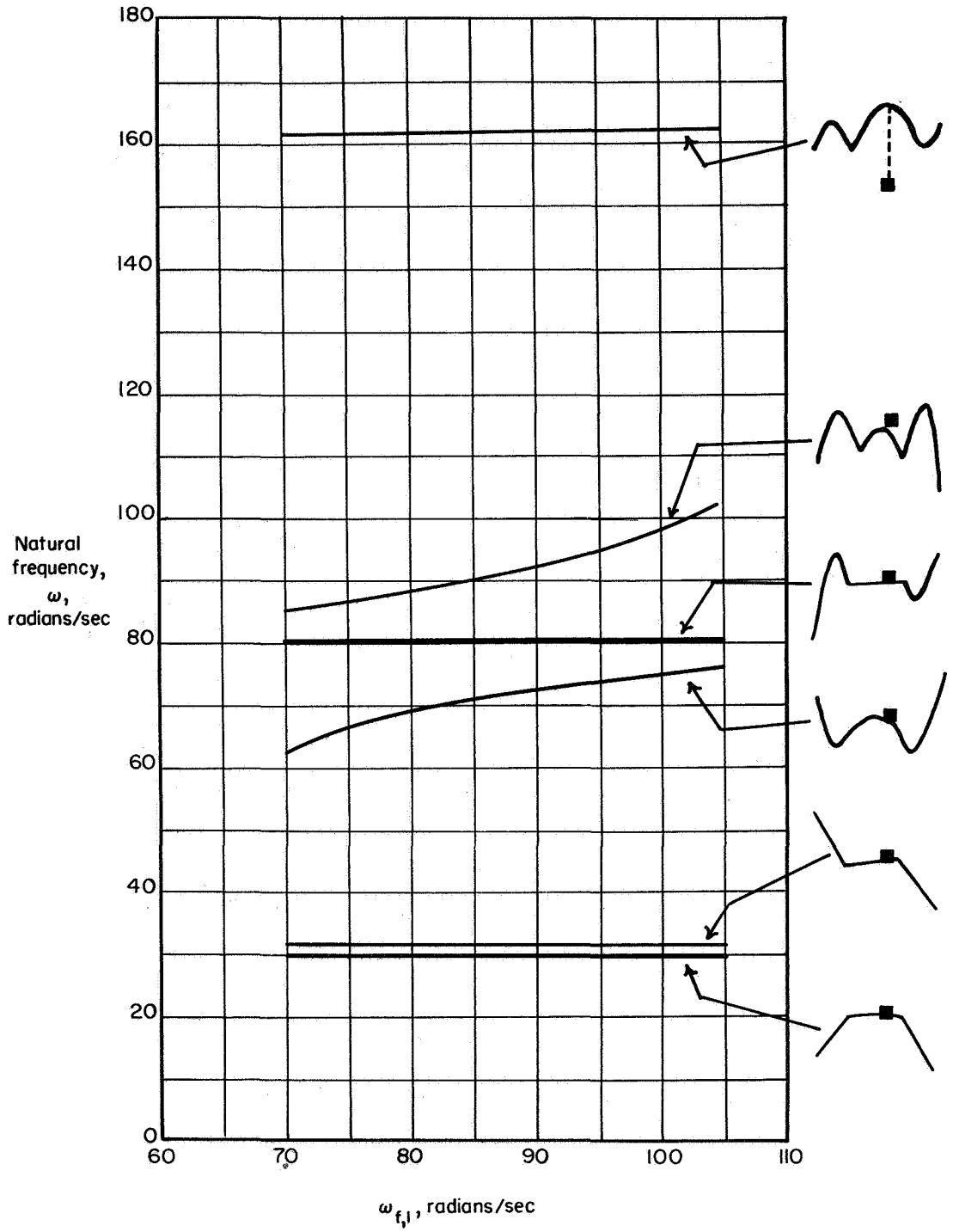

Figure 4.- Effect of natural uncoupled frequency of fuselage on natural frequencies of coupled system. Ω = 30 radians per second.

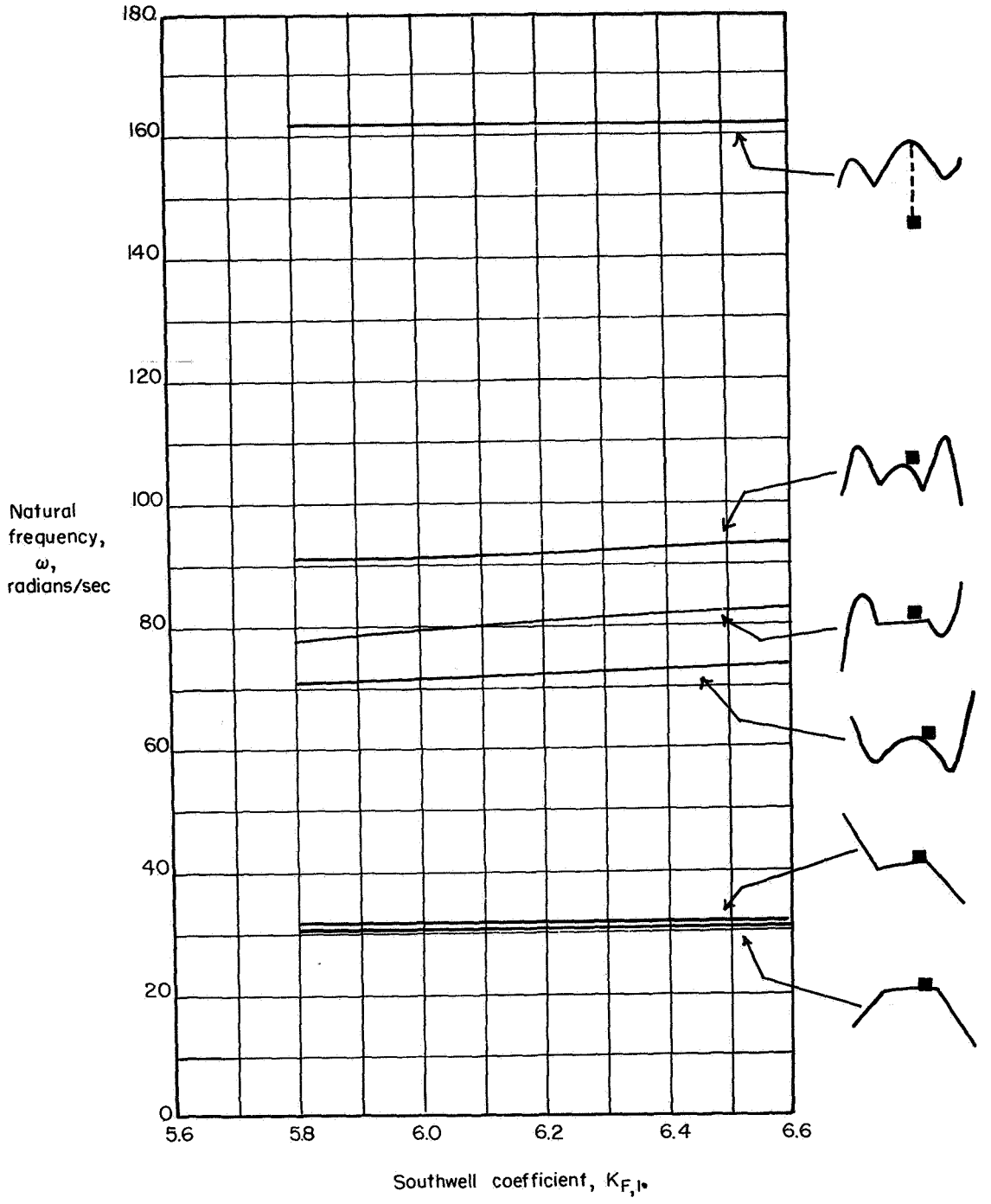

Figure 5.- Effect of Southwell coefficient for blade first elastic flapwise bending on natural frequencies of coupled system. Ω = 30 radians per second.

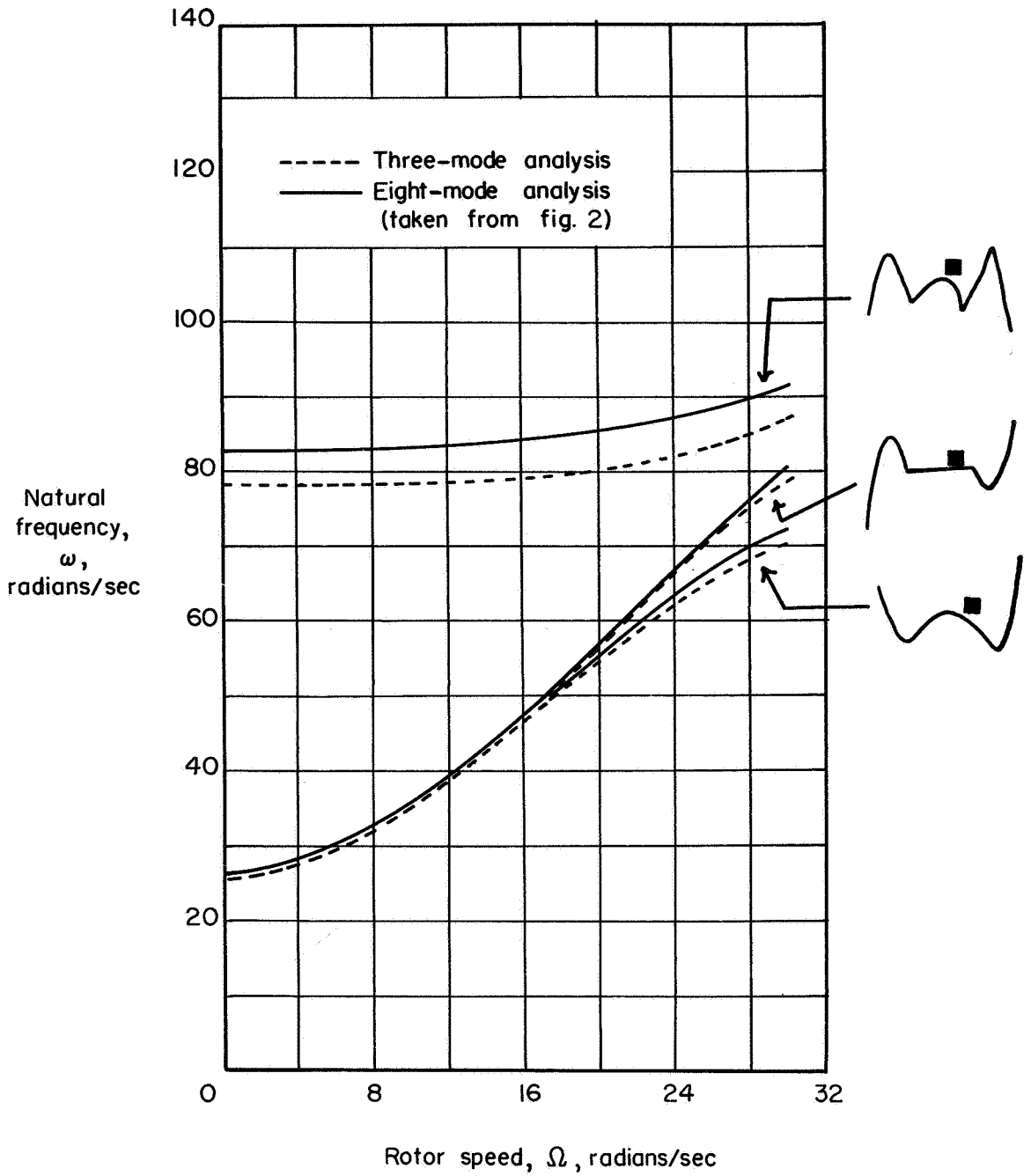

Figure 6.- Comparison of natural frequencies of coupled system from three-mode analysis with corresponding frequencies from eight-mode analysis.

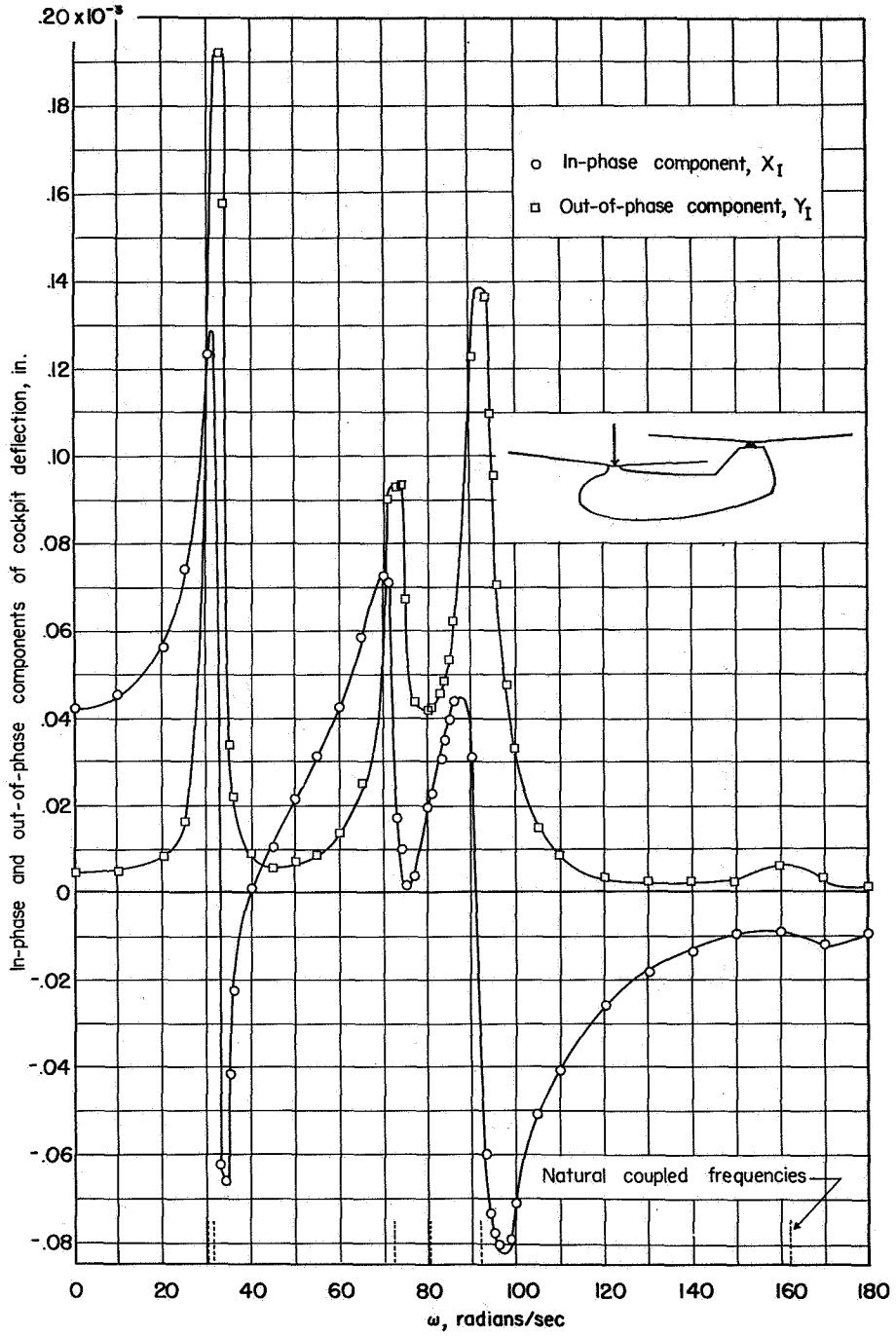

Figure 7.- Effect of forcing frequency on in-phase and out-of-phase components of amplitude of vibration of cockpit. Oscillating force of unit magnitude applied at front rotor hub.

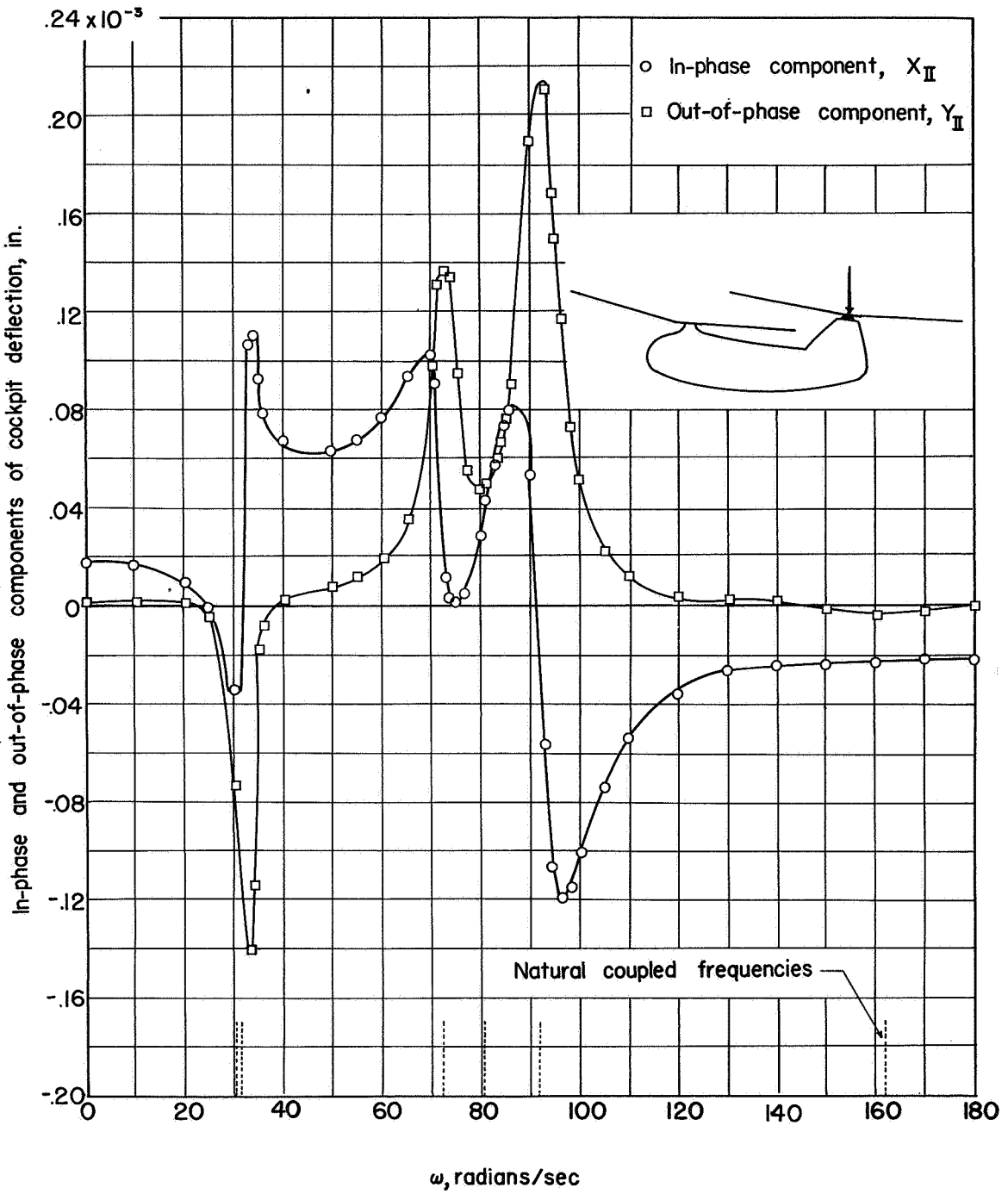

Figure 8.- Effect of forcing frequency on in-phase and out-of-phase components of amplitude of vibration of cockpit. Oscillating force of unit magnitude applied at rear rotor hub.

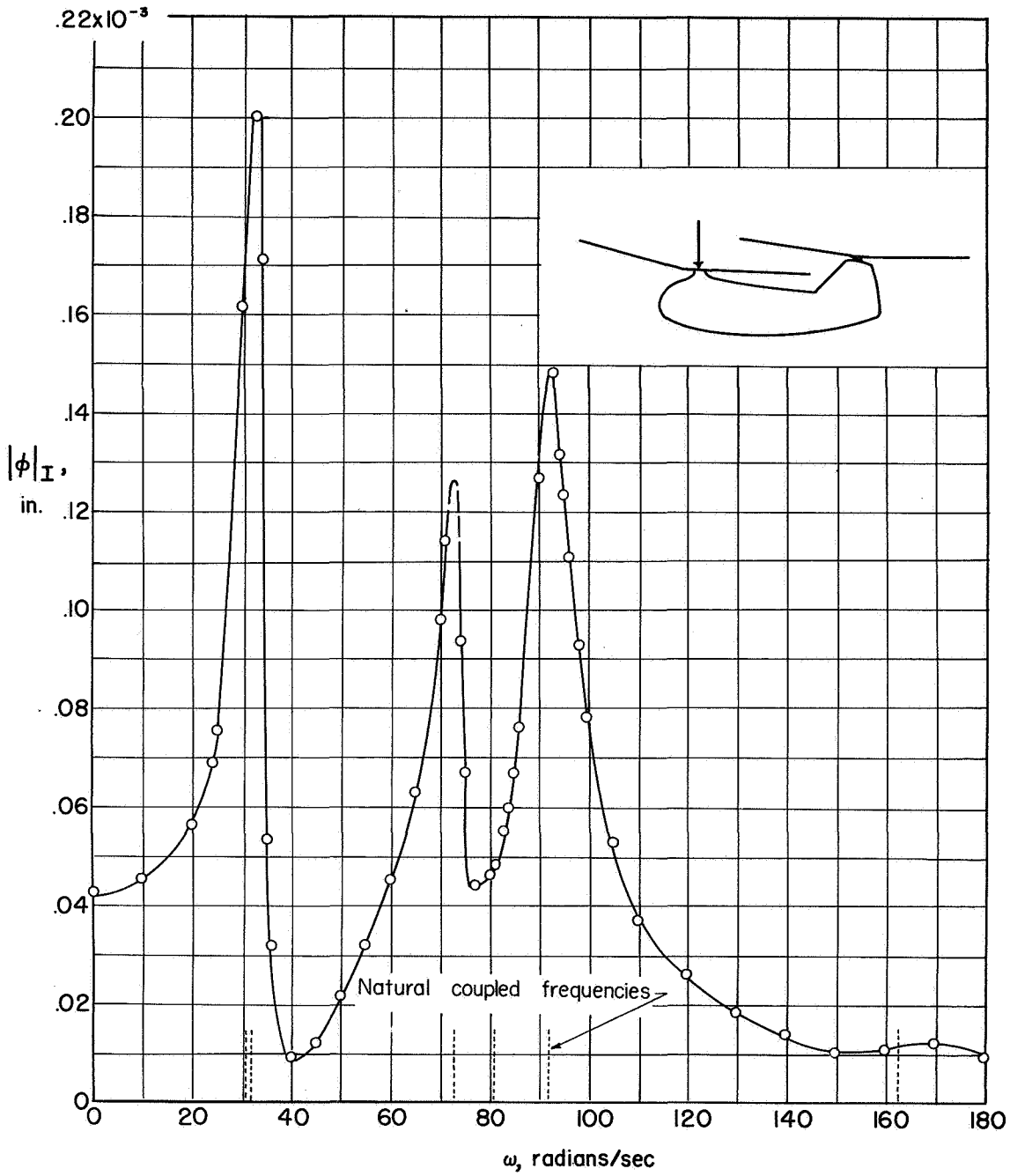

Figure 9.- Effect of forcing frequency on amplitude of vibration of cockpit. Oscillating force of unit magnitude applied at front rotor hub.

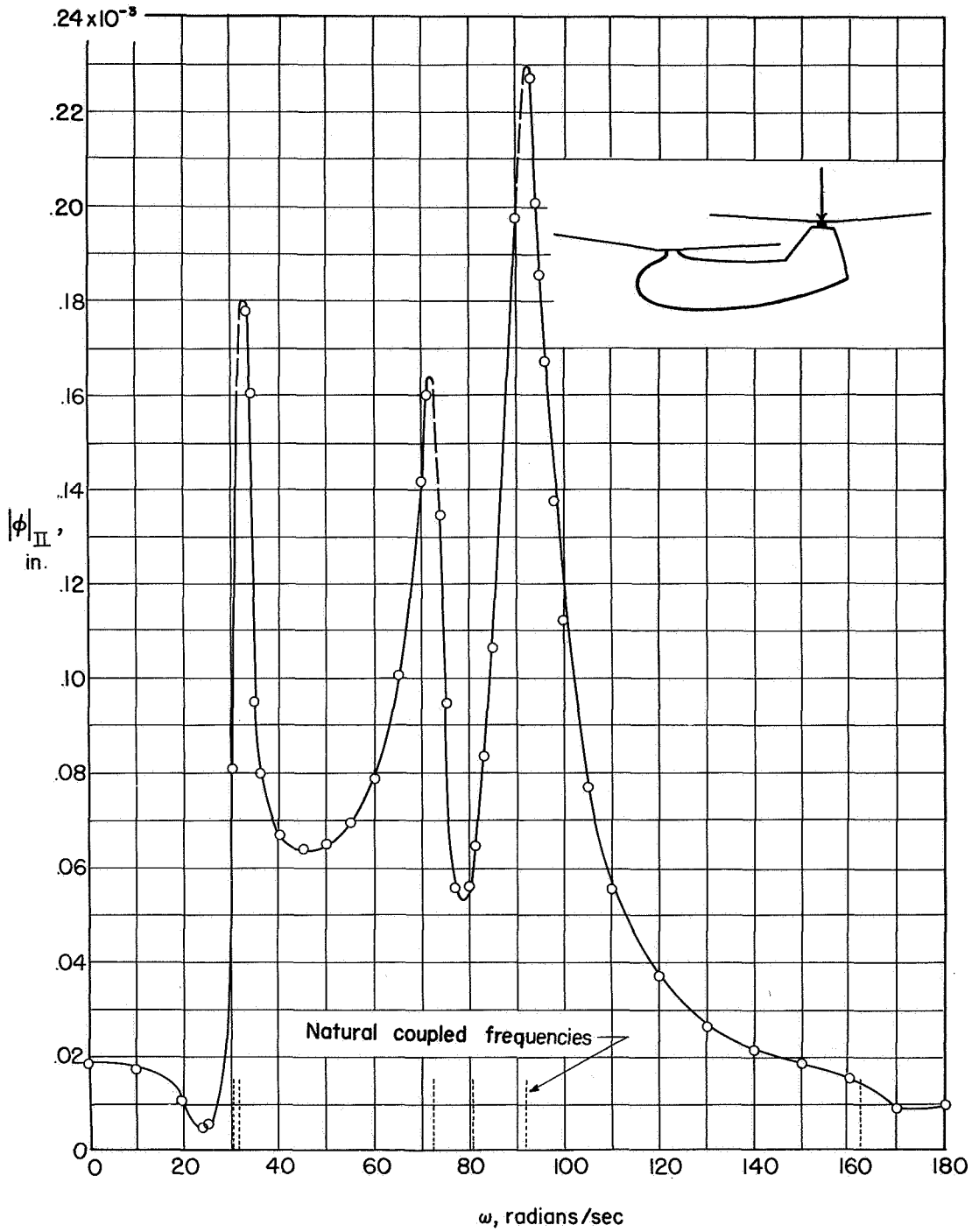

Figure 10.- Effect of forcing frequency on amplitude of vibration of cockpit. Oscillating force of unit magnitude applied at rear rotor hub.

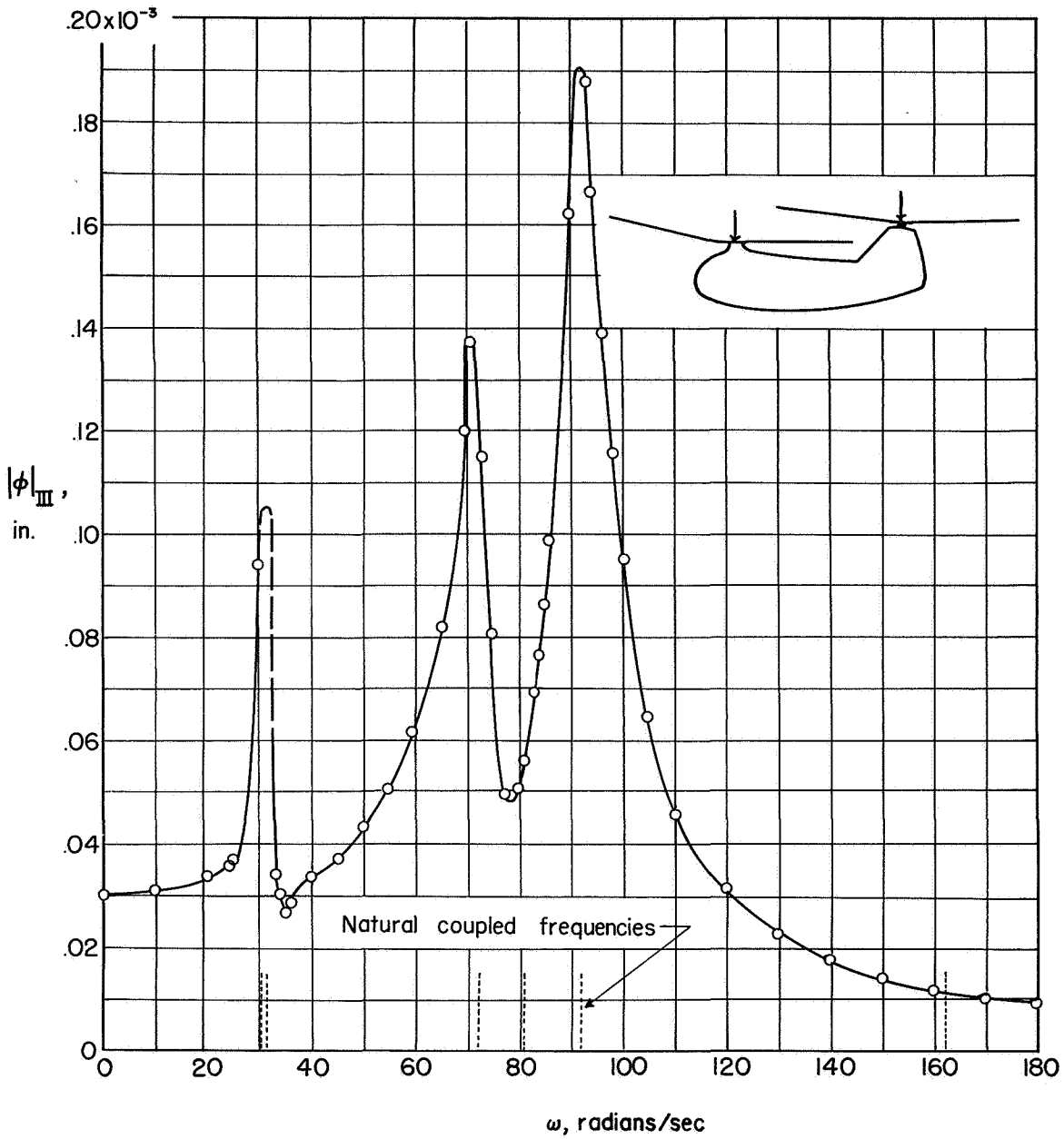

Figure 11.- Effect of forcing frequency on amplitude of vibration of cockpit. Oscillating force of unit magnitude equally divided between front and rear rotor hubs and applied in same direction.

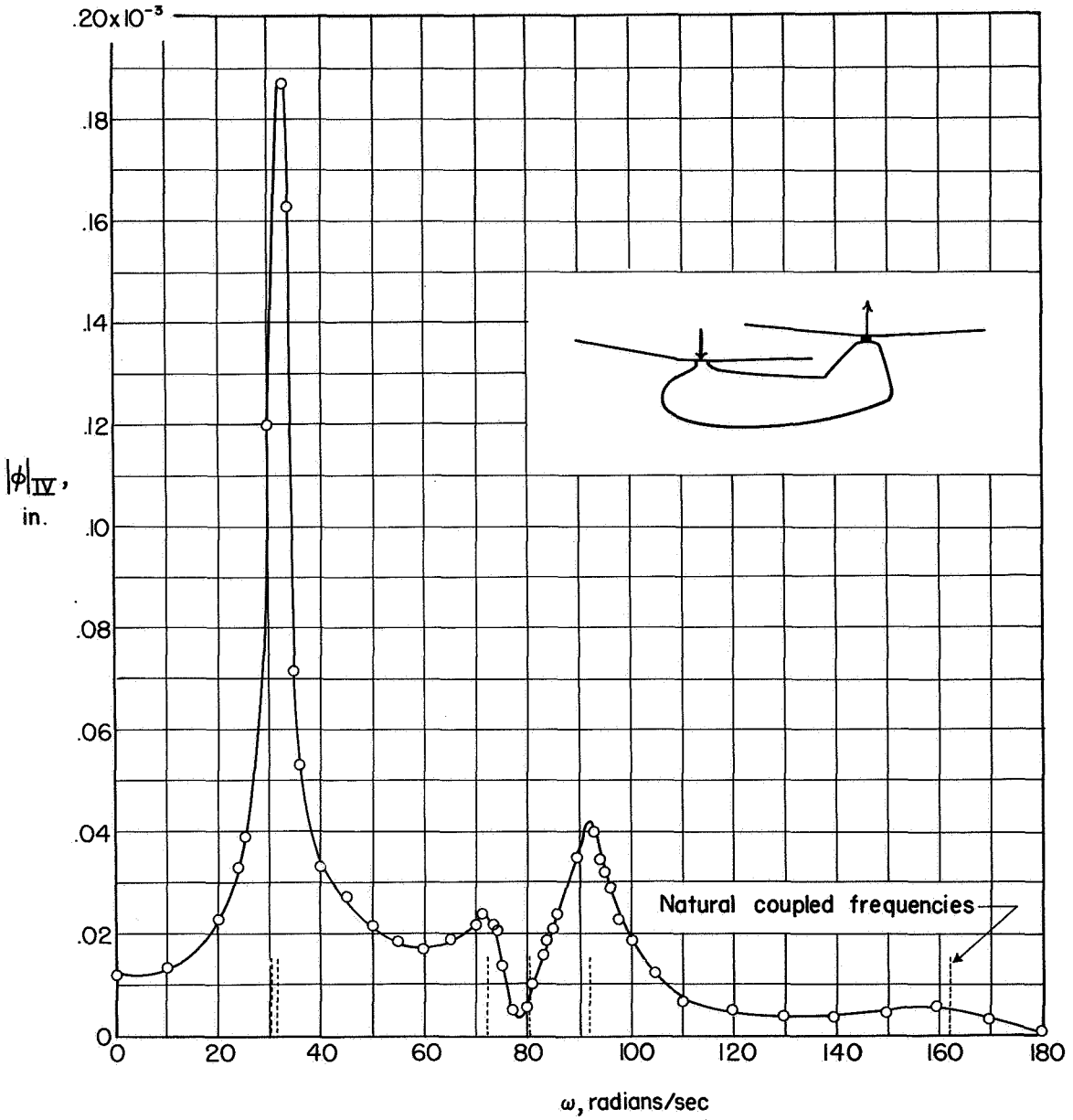

Figure 12.- Effect of forcing frequency on amplitude of vibration of cockpit. Oscillating force of unit magnitude equally divided between front and rear rotor hubs and applied in opposite directions.